Surface characterization techniques pdf

I'm not robot!

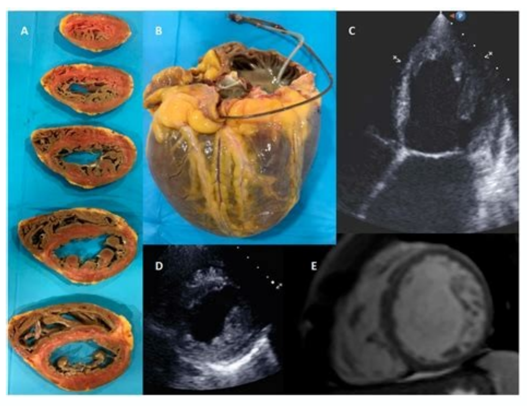

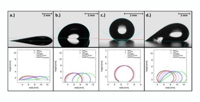

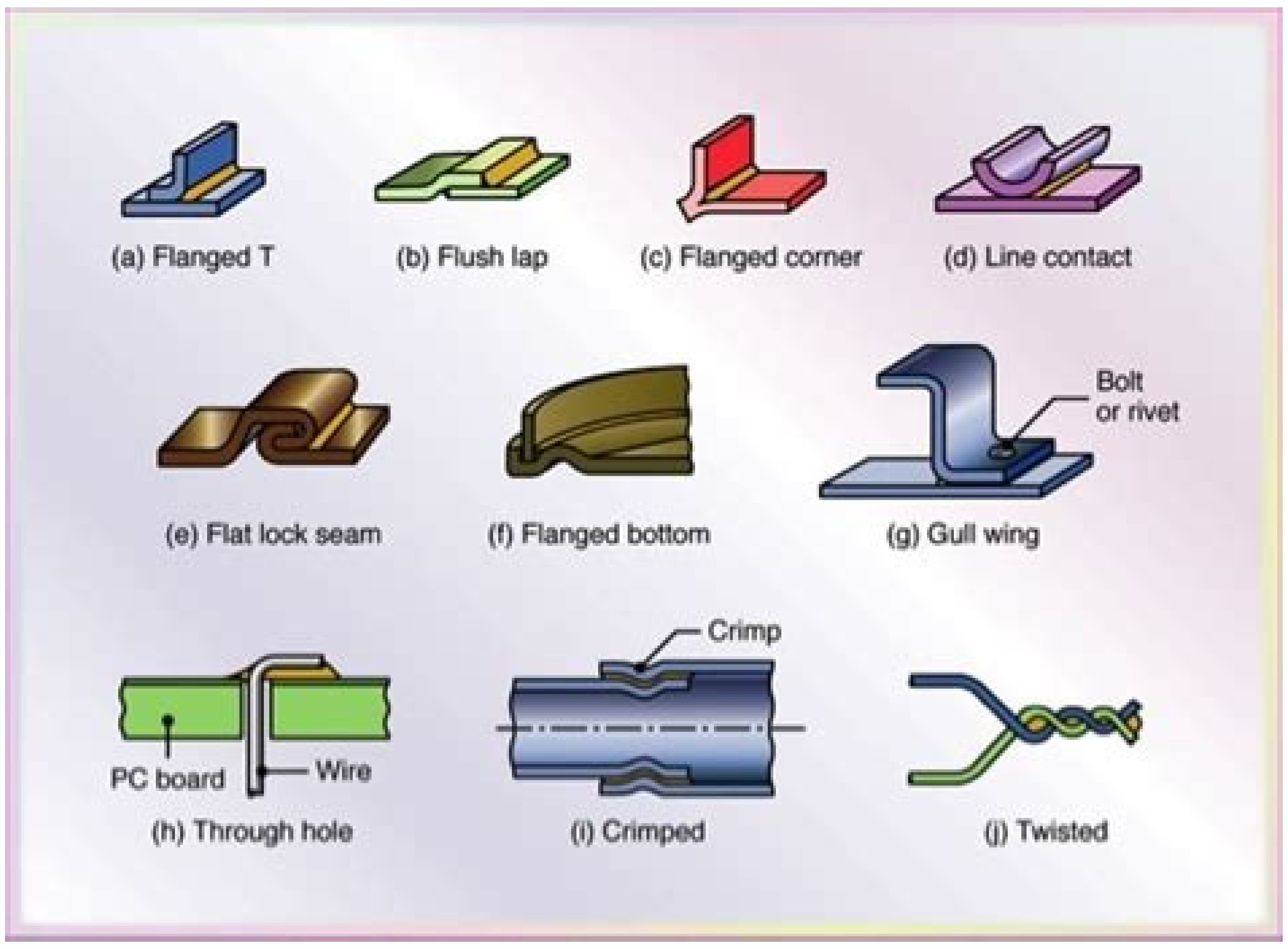

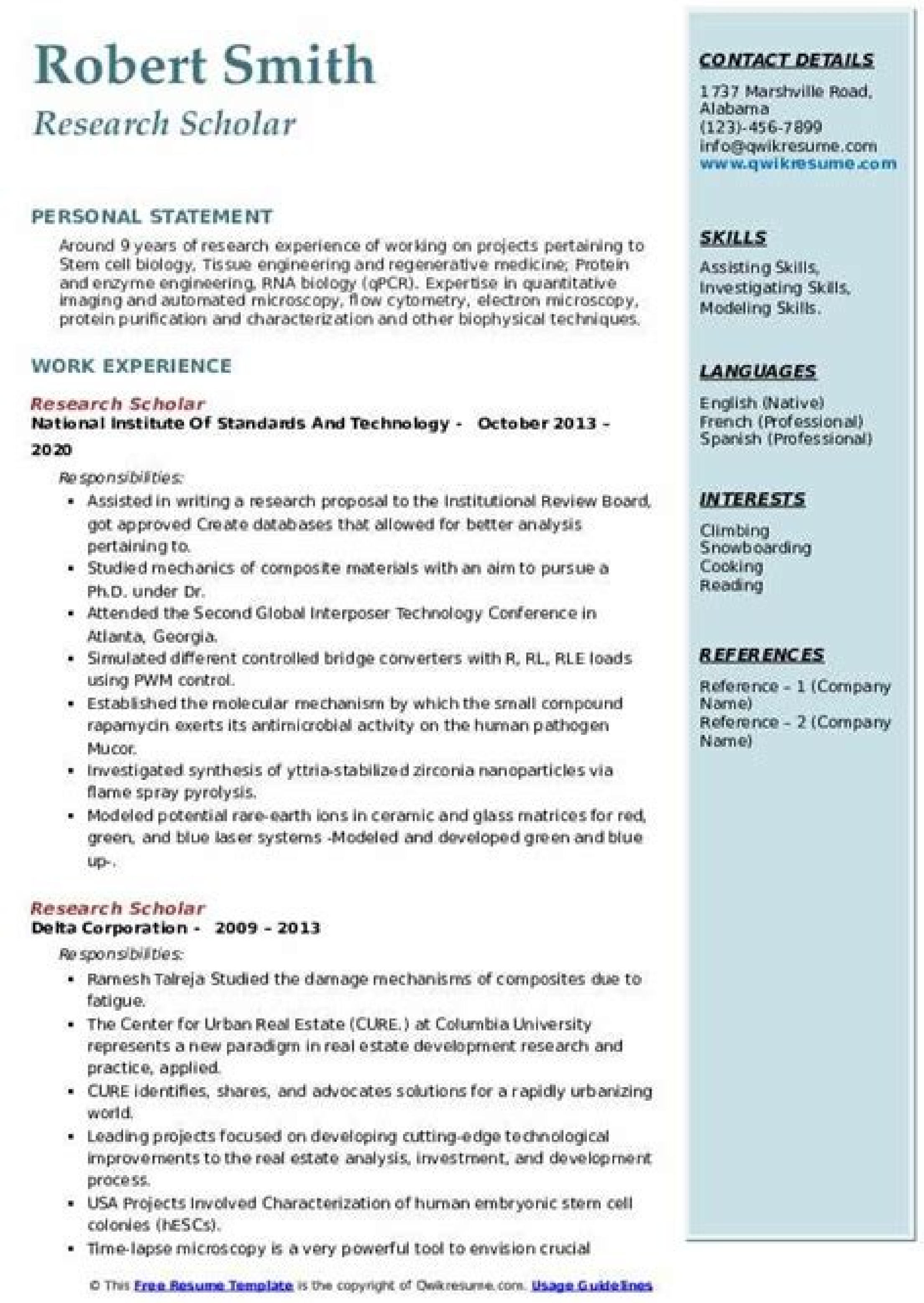

Robert Smith

Research Scholar

PERSONAL STATEMENT

Around 9 years of research experience of working on projects pertaining to Stem cell biology, Tissue engineering and regenerative medicine; Protein and enzyme engineering, RNA biology (qPCR). Expertise in quantitative imaging and automated microscopy, flow cytometry, electron microscopy, protein purification and characterization and other biophysical techniques.

WORK EXPERIENCE

Research Scholar
National Institute Of Standards And Technology - October 2013 - 2020

Responsibilities:

- Assisted in writing a research proposal to the Institutional Review Board, got approved Create databases that allowed for better analysis pertaining to.
- Studied mechanics of composite materials with an aim to pursue a Ph.D. under Dr.
- Attended the Second Global Interposer Technology Conference in Atlanta, Georgia.
- Simulated different controlled bridge converters with R, RL, RLE loads using PWM control.
- Established the molecular mechanism by which the small compound rapamycin exerts its antimicrobial activity on the human pathogen Mucor.
- Investigated synthesis of yttria-stabilized zirconia nanoparticles via flame spray pyrolysis.
- Modeled potential rare-earth ions in ceramic and glass matrices for red, green, and blue laser systems -Modeled and developed green and blue up-.

Research Scholar
Delta Corporation - 2009 - 2013

Responsibilities:

- Ramesh Talreja Studied the damage mechanisms of composites due to fatigue.
- The Center for Urban Real Estate (CURE.) at Columbia University represents a new paradigm in real estate development research and practice, applied.
- CURE identifies, shares, and advocates solutions for a rapidly urbanizing world.
- Leading projects focused on developing cutting-edge technological improvements to the real estate analysis, investment, and development process.
- USA Projects involved Characterization of human embryonic stem cell colonies (hESCs).
- Time-lapse microscopy is a very powerful tool to envision crucial

CONTACT DETAILS

1737 Marshville Road, Alabama
(123)-456-7899
info@qwikresume.com
www.qwikresume.com

SKILLS

Assisting Skills, Investigating Skills, Modeling Skills.

LANGUAGES

English (Native)
French (Professional)
Spanish (Professional)

INTERESTS

Climbing
Snowboarding
Cooking
Reading

REFERENCES

Reference – 1 (Company Name)
Reference – 2 (Company Name)

Surface characterization techniques pdf. Surface characterization methods. Surface and material characterization techniques. Surface characterization techniques ppt. Surface characterization techniques slideshare. Surface characterization techniques for polyurethane biomaterials. Surface and interface characterization techniques. Contact angle measurements and surface characterization techniques.

DOI: 10.1039/C8NR02278J (Review Article) Nanoscale, 2018, 10, 12871-12934Received 19th March 2018 , Accepted 4th June 2018First published on 4th June 2018Nanostructures have attracted huge interest as a rapidly growing class of materials for many applications. Several techniques have been used to characterize the size, crystal structure, elemental composition and a variety of other physical properties of nanoparticles. In several cases, there are physical properties that can be evaluated by more than one technique. Different strengths and limitations of each technique complicate the choice of the most suitable method, while often a combinatorial characterization approach is needed. In addition, given that the significance of nanoparticles in basic research and applications is constantly increasing, it is necessary that researchers from separate fields overcome the challenges in the reproducible and reliable characterization of nanomaterials, after their synthesis and further process (e.g. annealing) stages. The principal objective of this review is to summarize the present knowledge on the use, advances, advantages and weaknesses of a large number of experimental techniques that are available for the characterization of nanoparticles. Different characterization techniques are classified according to the concept/group of the technique used, the information they can provide, or the materials that they are destined for. We describe the main characteristics of the techniques and their operation principles and we give various examples of their use, presenting them in a comparative mode, when possible, in relation to the property studied in each case.Stefanos MourdikoudisDr Stefanos Mourdikoudis is a chemical engineer who obtained his PhD degree from the Department of Physics, Aristotle University of Thessaloniki in Greece in 2009. Apart from his native country, he also worked in post-doctoral projects in France and Spain. Currently he is working at the University College London (UCL) as a research associate. His current research activity involves mostly work on the synthesis and characterization of magnetic nanoparticles. The variety of nanostructures he prepares are either directed for specific applications or simply inspired from curiosity to explore new protocols and characterize the resulting products.Roger M. PallaresRoger M. Pallares received his BSc and MSc degrees in chemistry from the Ramon Llull University (Barcelona, Spain) in 2009 and 2011, respectively. After a year working on the growth of 2D nanomaterials at NTT Basic Research Laboratories (Atsugi, Japan), he started a joint doctoral program between the University College London (UCL, London, UK) and the Agency for Science, Technology and Research (Singapore), obtaining a PhD in materials science from UCL in 2016. He is currently a postdoctoral fellow at Northwestern University (Evanston, IL). His research interests focus on the use of nanomaterials for biomedical applications.Nguyen T. K. ThanhProfessor Nguyễn Thi Kim Thanh, FRSC, MInstP ( ), held a prestigious Royal Society University Research Fellowship (2005–2014). She was appointed a full professor in nanomaterials in 2013 at the Biophysics Group, Department of Physics and Astronomy, University College London, UK. She leads a very dynamic group conducting cutting edge interdisciplinary and innovative research on the design and synthesis of nanomaterials for biomedical applications from diagnostics to treatment of diseases such as cancer.She has published nearly 100 peer reviewed journal articles and book chapters with over 5000 citations so far. She has been a visiting professor at various universities in France, Japan, China and Singapore. She has been an invited speaker at over 200 institutes and scientific meetings. 1. Introduction Nanoscale materials often present properties different from their bulk counterparts, as their high surface-to-volume ratio results in an exponential increase of the reactivity at the molecular level. Such properties include electronic, optical and chemical properties, while the mechanical characteristics of the nanoparticles (NPs) may also differ extensively.1 This enables them to be an object of intensive studies due to their academic interest and the prospective technological applications in various fields. Such nanostructures may be synthesized by a wide number of methods, which involve mechanical, chemical and other pathways.2 Nowadays, many more types of nanomaterials are synthesized than only a decade ago, and in higher amounts than before, requiring the development of more precise and credible protocols for their characterization. However, such characterization is sometimes incomplete. This is because of the inherent difficulties of nanoscale materials to be properly analysed, compared to the bulk materials (e.g. too small size and low quantity in some cases following laboratory-scale production). In addition, the multidisciplinary aspects of nanoscience and nanotechnology do not permit every research team to have easy access to a broad range of characterization facilities. In fact, quite often a wider characterization of NPs is necessary, requiring a comprehensive approach, by combining techniques in a complementary way. In this context, it is desirable to know the limitations and strengths of the different techniques, in order to know if in some cases the use of only one or two of them is enough to provide reliable information when studying a specific parameter (e.g. particle size). Nanoscience and nanotechnology are still undergoing constant growth, and the scientific community is rather aware that there may be certain differences between the way analytical characterization methods operate for nanomaterials, in comparison with their more 'traditional' modes of use for more 'conventional' (macroscopic) materials.3 Herein we describe extensively the use of different methods for the characterization of NPs. These techniques are sometimes exclusive for the study of a particular property, while in other cases they are combined.4 We discuss all these techniques in a comparative way, considering factors such as their availability, cost, selectivity, precision, non-destructive nature, simplicity and affinity to certain compositions or materials. The techniques are analysed in depth, despite their big number presented herein. There are microscopy-based techniques (e.g. TEM, HRTEM, and AFM – the full names of the techniques are provided later in the text, when presenting each one of them), which provide information on the size, morphology and crystal structure of the nanomaterials. Other techniques are specialized for certain groups of materials, such as the magnetic techniques. Examples of these techniques are SQUID, VSM, FMR, and XMCD. Many other techniques provide further information on the structure, elemental composition, optical properties and other common and more specific physical properties of the nanoparticle samples. Examples of these techniques include X-ray, spectroscopy and scattering techniques. This review is organized in different sections, which will present numerous distinct characterization techniques for NPs in relation to the properties studied (see Tables 1 and 2). The sections are categorized according to the different technique groups, as described above. Table 1 Summary of the experimental techniques that are used for nanoparticle characterization featured in this paper Technique Main information derived Section Fig. XRD (group: X-ray based techniques) Crystal structure, composition, crystalline grain size 2.1 XAS (EXAFS, XANES) X-ray absorption coefficient (element-specific) – chemical state of species, interatomic distances, Debye–Waller factors, also for non-crystalline NPs 2.1 SAXS Particle size, size distribution, growth kinetics 2.1 1 XPS Electronic structure, elemental composition, oxidation states, ligand binding (surface-sensitive) 2.1 FTIR (group: further techniques for structure/composition/main properties) Surface composition, ligand binding 2.2 NMR (all types) Ligand density and arrangement, electronic core structure, atomic composition, influence of ligands on NP shape, NP size 2.2 BET Surface area 2.2 TGA Mass and composition of stabilizers 2.2 LEIS Thickness and chemical composition of self-assembled monolayers of NPs 2.2 UV-Vis Optical properties, size, concentration, agglomeration state, hints on NP shape 2.2 PL spectroscopy Optical properties – relation to structure features such as defects, size, composition 2.2 DLS Hydrodynamic size, detection of agglomerates 2.2 2 NTA NP size and size distribution 2.2 3 DCS NP size and size distribution 2.2 ICP-MS Elemental composition, size, size distribution, NP concentration 2.2 4 SIMS, ToF-SIMS, MALDI Chemical information (surface-sensitive) on functional group, molecular orientation and conformation, surface topography, MALDI for NP size 2.2 5 RMM-MEMS, ζ-potential, pH, EPM, GPC, DSC, etc. Please check the relevant parts of the manuscript 2.2 SQUID-nanoSQUID (group: magnetic nanomaterials) Magnetization saturation, magnetization remanence, blocking temperature 2.3 6 VSM Similar to SQUID through M–H plots and ZFC-FC curves 2.3 Mössbauer Oxidation state, symmetry, surface spins, magnetic ordering of Fe atoms, magnetic anisotropy energy, thermal unblocking, distinguish between iron oxides 2.3 7 FMR NP size, size distribution, shape, crystallographic imperfection, surface composition, M values, magnetic anisotropic constant, demagnetization field 2.3 XMCD Site symmetry and magnetic moments of transition metal ions in ferro- and ferri-magnetic materials, element specific 2.3 Magnetic susceptibility, magnetophoretic mobility Please check the relevant parts of the manuscript 2.3 Superparamagnetic relaxometry Core properties, hydrodynamic size distribution, detect and localize superparamagnetic NPs 2.3 8 TEM (group: microscopy techniques) NP size, size monodispersity, shape, aggregation state, detect and localize/quantify NPs in matrices, study growth kinetics 2.4 9 and 10 HRTEM All information by conventional TEM but also on the crystal structure of single particles. Distinguish monocrystalline, polycrystalline and amorphous NPs. Study defects 2.4 11 and 12 Liquid TEM Depict NP growth in real time, study growth mechanism, single particle motion, superlattice formation 2.4 13 Cryo-TEM Study complex growth mechanisms, aggregation pathways, good for molecular biology and colloid chemistry to avoid the presence of artefacts or destroyed samples 2.4 14 Electron diffraction Crystal structure, lattice parameters, study order–disorder transformation, long-range order parameters 2.4 STEM Combined with HAADF, EDX for morphology study, crystal structure, elemental composition. Study the atomic structure of hetero-interfaces 2.4 Aberration-corrected (STEM, TEM) Atomic structure of NP clusters, especially bimetallic ones, as a function of composition, alloy homogeneity, phase segregation 2.4 15 and 16 EELS (EELS-STEM) Type and quantity of atoms present, chemical state of atoms, collective interactions of atoms with neighbors, bulk plasmon resonance 2.4 17 Electron tomography Realistic 3D particle visualization, snapshots, video, quantitative information down to the atomic scale 2.4 18 and 19 SEM-HRSEM, T-SEM-EDX Morphology, dispersion of NPs in cells and other matrices/supports, precision in lateral dimensions of NPs, quick examination–elemental composition 2.4 20 EBSD Structure, crystal orientation and phase of materials in SEM. Examine microstructures, reveal texture, defects, grain morphology, deformation 2.4 AFM NP size and shape in 3D mode, evaluate degree of covering of a surface with NP morphology, dispersion of NPs in cells and other matrices/supports, precision in lateral dimensions of NPs, quick examination–elemental composition 2.4 21, 22 and 23 MFM Standard AFM imaging together with the information of magnetic moments of single NPs. Study magnetic NPs in the interior of cells. Discriminate from non-magnetic NPs 2.4 21 Table 2 Parameters needed to be determined and the corresponding characterization techniques Entity characterized Characterization techniques suitable Size (structural properties) TEM, XRD, DLS, NTA, SAXS, HRTEM, SEM, AFM, EXAFS, FMR, DCS, ICP-MS, UV-Vis, MALDI, NMR, TRPS, EPLS, magnetic susceptibility Shape TEM, HRTEM, AFM, EPLS, FMR, 3D-tomography Elemental-chemical composition XRD, XPS, ICP-MS, ICP-OES, SEM-EDX, NMR, MFM, LEIS Crystal structure XRD, EXAFS, HRTEM, electron diffraction, STEM Size distribution DCS, DLS, SAXS, NTA, ICP-MS, FMR, superparamagnetic relaxometry, DTA, TRPS, SEM Chemical state–oxidation state XAS, EELS, XPS, Mössbauer Growth kinetics SAXS, NMR, TEM, cryo-TEM, liquid-TEM Ligand binding/composition/density/arrangement/mass, surface composition XPS, FTIR, NMR, SIMS, FMR, TGA, SANS Surface area, specific surface area BET, liquid NMR Surface charge Zeta potential, EPM Concentration ICP-MS, UV-Vis, RMM-MEMS, PTA, DCS, TRPS Agglomeration state Zeta potential, DLS, DCS, UV-Vis, SEM, Cryo-TEM, TEM Density DCS, RMM-MEMS Single particle properties Sp-ICP-MS, MFM, HRTEM, liquid TEM 3D visualization 3D-tomography, AFM, SEM Dispersion of NP in matrices/supports SEM, AFM, TEM Structural defects HRTEM, EBSD Detection of NPs TEM, SEM, STEM, EBSD, magnetic susceptibility Optical properties UV-Vis-NIR, PL, EELS-STEM Magnetic properties SQUID, VSM, Mössbauer, MFM, FMR, XMCD, magnetic susceptibility 2. Characterization of nanoparticles Two of the main parameters studied in the characterization of NPs are size and shape. We can also measure size distribution, degree of aggregation, surface charge and surface area, and to some extent evaluate the surface chemistry.5 Size, size distribution and organic ligands present on the surface of the particles may affect other properties and possible applications of the NPs. In addition, the crystal structure of the NPs and their chemical composition are thoroughly investigated as a first step after nanoparticle synthesis. Until now, there were no standardized protocols for this aim. Credible and robust measurement methods for NPs will greatly affect the uptake of these materials in commercial applications and allow the industry to comply with regulation. Nevertheless, there are important challenges in the analysis of nanomaterials because of the interdisciplinary nature of the field, the absence of suitable reference materials for the calibration of analytical tools, the difficulties linked to the sample preparation for analysis and the interpretation of the data. In addition, there are unmet challenges in the characterization of NPs such as the measurement of their concentration in situ and on-line, especially in a scaled-up production, as well as their analysis in complex matrices. Waste and effluent from mass production will also need to be monitored.6 With the scale-up of nanoparticle manufacture, more reliable quantification techniques will be required. For this reason, it is crucial to characterize the nanomaterials prepared in several ways to the maximum extent. We do not only focus on the characterization of the nanoparticle core, but also on the surface ligands that influence the physical properties. In addition, we do not present only techniques that one might classify as 'common', but we also show examples of modern in situ operando techniques that are used to monitor the kinetics of nanoparticle formation and study through some recent advances in the topic the controlled defects that affect nanoparticle properties in a crucial manner. 2.1 X-ray-based techniques X-ray diffraction (XRD) is one of the most extensively used techniques for the characterization of NPs. Typically, XRD provides information regarding the crystalline structure, nature of the phase, lattice parameters and crystalline grain size. The latter parameter is estimated by using the Scherrer equation using the broadening of the most intense peak of an XRD measurement for a specific sample. An advantage of the XRD techniques, commonly performed in samples of powder form, usually after drying their corresponding colloidal solutions, is that it results in statistically representative, volume-averaged values. The composition of the particles can be determined by comparing the position and intensity of the peaks with the reference patterns available from the International Centre for Diffraction Data (ICDD, previously known as Joint Committee on Powder Diffraction Standards, JCPDS) database. However, it is not suitable for amorphous materials and the XRD peaks are too broad for particles with a size below 3 nm. Upadhyay et al. determined the average crystallite size of magnetite NPs using X-ray line broadening, and it was found to be in the range of 9–53 nm. The broadening of XRD peaks was mainly caused by particle/crystallite size and lattice strains other than instrumental broadening.7 The XRD-derived size is usually bigger than the so-called magnetic size, due to the fact that smaller domains are present in a particle where all moments are aligned in the same direction, even if the particle is single domain. On the contrary, the TEM-deduced size was higher than that calculated using XRD, for samples with very large particles; in fact, when the particle size is bigger than 50 nm, there are more than one crystal boundary on their surface. XRD cannot distinguish between the two boundaries; therefore the actual (TEM) size of certain samples can be in reality bigger than the 50–55 nm calculated by the Scherrer formula. Dai and co-workers prepared ultra-small Au NPs which were very likely to be more developed along the 111 direction (rather than the 220 one) as the peak corresponding to the former direction was much more intense in their XRD measurement.8 Similarly, Li and colleagues noticed that after preparing copper telluride nanostructures with different shapes (i.e. cubes, plates, and rods), the relative intensities between the different XRD peaks varied in relation to the particle shape.9 X-ray absorption spectroscopy (XAS) includes both extended X-ray absorption fine structure (EXAFS) and X-ray absorption near edge structure (XANES, also known as NEXAFS). XAS measures the X-ray absorption coefficient of a material as a function of energy. Each element has a set of characteristic absorption edges corresponding to the different binding energies of its electrons, giving XAS element selectivity. As a highly sensitive technique, EXAFS is a convenient way to identify the chemical state of species which may occur even in very low concentrations. Synchrotrons are usually needed to acquire XAS spectra; therefore it is not a routine or readily available technique. XANES probes the density of states of empty/partially filled electronic states by considering the excitation of an inner shell electron to those states that are permitted by dipole selection rules. Pugsley et al. used in situ XAS to examine the kinetics and mechanism of formation of germanium NPs upon the reaction of Mg_2Ge and $GeCl_4$.10 Actually, the EXAFS experiments and TEM results indicated the formation of GeO_2 NPs along with the Ge NPs. The analysis of EXAFS yielded a first-neighbour Ge–Ge distance of 2.45 Å in good agreement with XRD. Moreover, Chen et al. applied in situ EXAFS for the inspection of structural changes around germanium atoms in GeO_2 NPs. Surprisingly, they noticed that at high temperature GeS_2 was formed as a product of the complete transformation of germanium dioxide, in the presence of a sulfur source.11 Requejo and co-workers investigated the effects of sulfur–palladium interaction on the structural and electronic properties of alkyl thiol-capped Pd NPs. The XANES and EXAFS analyses of the atomic structure and electronic properties of these NPs showed that the sulfidation of Pd clusters caused by the capping thiol molecules took place not only on the surface but also in the bulk.12 Energy dispersive EXAFS helps to determine both structural and kinetic parameters in supported metal catalysts for reactions occurring on a timescale of a few seconds. Such a fast operation enables the aforementioned technique to be used at temperatures higher than 200 °C, which would hinder the use of surface enhanced Raman spectroscopy (SERS), as the latter technique is not that fast under such conditions. Even on a timescale of tens of milliseconds, energy dispersive EXAFS can be used as a quantitatively suitable in situ probe of the dynamics of quick phase change in supported nanoparticulate metal catalysts.13 Bugaev and colleagues determined with EXAFS parameters the atomic structure of PtCu NPs in PtCu/C catalysts. EXAFS is one of the most convenient techniques for the structural analysis of NPs with sizes lower than 10 nm. It possesses a high spatial resolution and provides information on the nearest environment of an atom in a compound in the absence of long-range order. The parameters derived in that study were partial coordination numbers, interatomic distances and Debye–Waller factors.14 Moreover, Klasovsky and co-workers performed a physicochemical characterization of a new electron-conducting polymer (PANI) supported PtO_2 catalyst by electron paramagnetic resonance (EPR), diffuse reflectance FTIR spectroscopy (DRIFTS) and EXAFS. The importance of in situ/operando techniques was highlighted toward a better comprehension of the working oxidation catalyst.15 In another study, Zhang and colleagues coated γ-Fe_2O_3 NPs with sodium dodecylbenzene sulphonate (DBS), stearic acid and hexadecyltrimethylammonium bromide (CTAB) surfactants by the microemulsion method. The role of the surfactants was investigated through EXAFS analysis and it was found that all samples had a tendency to extend the Fe–O bond length. All these molecules possess large spatial resistance, with the CTAB molecule having the largest one. The lattice distortion and disorder at the interfaces could play a significant role in hindering the fast nanoparticle growth.16 $CuFe_2O_4$ and $CuFe_2O_4$–MO_2 (M = Sn, Ge) NPs were investigated by Bertagnolli and colleagues by means of EXAFS and XANES. The authors state the importance of EXAFS for the acquisition of information concerning the coordination number, the nature of the scattering atoms surrounding the absorbing atom, the interatomic distance between absorbing and backscattering atoms, as well as the Debye–Waller factor, which is related to a disorder because of static displacements and thermal vibrations.17 The Fourier transform (FT) of the EXAFS signal as a function of wavenumber is related to the radial distribution of backscattering atoms in real space x(r). The possible phase shifts during the EXAFS process and interference effects from different scattering channels cause the modification of the position of the peaks in the FT, which become no longer identical to the geometric distance between the backscattering atoms and the absorbing atom. As an alternative method aiming to tackle the drawbacks of the FT approach, the wavelet transform (WT) has been proposed, as reported by C. Schmitz Antoniak.18 The principal concept behind the WT is to replace the infinitely expanded periodic oscillations in a FT with located wavelets as a kernel for the integral transformation. More details of that approach can be found in ref. 18. EXAFS can also be used to study copper cation inversion in $CuFe_2O_4$ as a function of saturation magnetization. XANES is more helpful to determine the oxidation states, vacant orbitals, electronic configuration and site symmetry of the absorbing atom. XANES measurements were in agreement with EXAFS, both suggesting that iron (Fe) ions occupied more tetrahedral sites than octahedral sites. Overall, these researchers showed that the aforementioned investigation on their copper ferrite NPs illustrated that these nanostructures had a structure analogous to that of the corresponding bulk material. The incorporation of the tetravalent metal ions in the spinel structures did not modify the local environment around Cu and Fe ions.17 Moroz reviewed the X-ray diffraction structure diagnostics of nanomaterials and stated that a remarkable advantage of EXAFS over REDD (radial electron density distribution) is its selectivity, whereas REDD is better in providing accurate values of the interatomic distances; in that case, EXAFS provides interatomic distances corrected for the phase shift. Ideally, REDD should be combined with EXAFS, FTIR and microscopy techniques to acquire knowledge on the relation between the structure and physicochemical properties of nanomaterials.19 In another work, Gomes et al. combined XRD and EXAFS to determine the cation distribution and other structural parameters, comparing the NP-based sample spectrum with the standard bulk material spectrum of the Cu ferrite. Differences were found among the cation redistribution at the nanoparticle samples with regard to the ideal copper ferrite.20 CeO_2 NPs were characterized with EXAFS by Zhu and co-workers. The authors emphasized on the suitability of the technique under discussion for their materials due to its element selectivity and nondependence on the long-range order of materials. From the acquired Debye–Waller factors and the Ce–O bond lengths, it was deduced that the surface or interface of the NPs coated with sodium bis(2-ethylhexyl) sulfosuccinate (AOT) surfactants was quite ordered; however the bond lengths were elongated.21 Swatsitang and colleagues analysed with EXAFS the impact of cation distribution on the magnetic properties of $Co_{1-x}Ni_xFe_2O_4$ NPs prepared by a hydrothermal method. The results implied that Co and Ni ions could occupy both the tetrahedral and octahedral sites with the preference to occupy the octahedral site more than the tetrahedral site, which is different from the bulk sample where all cations occupy only the octahedral site in an inverse spinel ferrite model structure.22 Furthermore, Zhang et al. synthesized Co@SiO_2 core–shell NPs with the sol–gel approach. In situ XRD was used along with EXAFS to monitor the oxidation process of the Co cores after thermal treatment at 800 °C either in air or under an inert atmosphere. Interestingly, it was noticed that Co was oxidized in three steps no matter if air or N_2 gas was employed during the annealing.23 Ni–P was another material in nanoscale form studied by EXAFS. In particular, EXAFS proved to be very robust for the screening of the initial crystallization behaviour of such amorphous NPs by probing the atomic-level structural change. Its combination with XRD, HRTEM and VSM helped to investigate in detail the structural changes of Ni–P NPs in both short-range and long-range order during heating at high temperatures. More specifically, XRD illustrated the crystalline phases and phase changes. HRTEM provided information on size, size distribution and shape. EXAFS provided insights regarding the changes of a local atomic structure and the chemical valence, especially for XRD-amorphous samples. VSM enabled the study of magnetic properties corresponding to different crystallization stages.24 Metal chalcogenides have also been analysed by EXAFS, as in the case of CdS NPs prepared by Rockenberger et al.25 They found EXAFS to be suitable for their samples since it does not rely on any long-range order, in contrast to XRD. EXAFS can also be used for liquid samples or even in cluster beams in the gaseous phase, permitting the identification of intercluster interactions by comparison with solid state measurements. It revealed that the stabilization of CdS NPs with 1.3–12 nm diameter affected the mean Cd–S distance. Unlike XRD, EXAFS is only sensitive to the local geometrical arrangement of neighboring atoms that surround the absorbing atom. O'Brien and colleagues investigated the local environment of phosphorus in the capping agent on the surface of CdSe quantum dots. The binding mode of the capping agents onto the surface was analysed, depending on the use of two distinct synthetic routes followed for its preparation (ligands: trioctylphosphine oxide and/or trioctylphosphine selenide).26 Furthermore, Lloyd and co-workers used various techniques, including EXAFS, to monitor the reduction of Se(IV) to Se(II) by a microbial whole-cell catalyst (Veillonella atypica). The reduction was found to proceed via an insoluble red amorphous Se(0) phase and the formation of metal selenide was shown by EXAFS analysis from both ex situ and in situ ways.27 Noble metal nanostructures, either monometallic or bimetallic, have also been studied by EXAFS. For example, the structural features of silver NPs embedded in silicate glass were investigated combining HRTEM and EXAFS techniques.28 Bugaev's group employed HRTEM, XRD, optical absorption and EXAFS to identify correlations between the plasmonic properties and the atomic structure of Ag NPs and their aggregates. The processing of the Ag K-edge EXAFS spectra resulted in the acquisition of values for the parameters of the atomic structure in Ag–Ag and Ag–O bonds averaged over the ionic and neutral states of Ag.29 The determination of the atomic structure of metallic Ag NPs, such as the type of point symmetry in the interior (core) region of small NPs, the nearest-neighbor Ag–Ag distances and the structure of the near-surface region, is a challenging problem for this system. The same group analysed by EXAFS the changes in the atomic structure of Ag NPs in soda-lime glass after annealing at 550 °C for 8 h.30 Brunsch and co-workers found that EXAFS showed a higher accuracy than HRTEM in the determination of lattice parameters for Ag NPs embedded in silicate glasses. The EXAFS results were averaged parameters of atom–atom correlations summed up for all detected particles, different from the data derived by HRTEM for single particles. Combining both techniques would be beneficial for precise structural characterization.31 The same researchers achieved the determination of the thermal expansion coefficient of similar glass-embedded silver NPs, in a wide range of temperatures. EXAFS allowed the precise demonstration of the changes of bond lengths and the stress state of their materials on the basis of a thermal expansion mismatch. The evaluation of the EXAFS data of small NPs typically provides a decreased coordination number, a dilatation or a contraction of the lattice structure and an increased Debye–Waller factor, together with an increased static disorder.32 In addition, EXAFS does not require operation under vacuum, in contrast to XPS. It was used by the Parkin group to investigate the phase change in silver speciation, during the photo-assisted growth of Ag from $AgNO_3$.33 The most plausible transition from metallic silver to Ag_2O was illustrated. EXAFS has also been applied for the characterization of alloys such as Pd_xPt_y NPs since common analytical techniques, such as XRD, have a limited capacity to distinguish between the various compositions of the aforementioned alloy, i.e. these metals are perfectly miscible in any relative proportion and they both possess an fcc structure with similar lattice constants. Furthermore, structural information can also be obtained from EXAFS measurements, even though sometimes with lower precision and difficulty in extraction in comparison with the use of XRD.34 Ingham has written a comprehensive review describing what X-ray scattering techniques such as EXAFS, in situ XRD and small-angle X-ray scattering (SAXS) can offer in nanoparticle characterization.35 Beale and Weckhuysen have reported how the ratio between coordination numbers varied as a function of shape, through the EXAFS data. Their study concerned a series of nanoscale structures with several shapes and fcc, hcp, or bcc structures, with a maximum isotropic diameter of 3 nm.36 In the case of Pt–Ru nanoclusters, size could also be obtained from EXAFS analysis, due to the fact that the coordination number of nearest neighbors in NPs is a non-linear function of the particle diameter if the latter parameter lies below the range of 3–5 nm.37 Sokolov and co-workers characterized their Pd NPs – synthesized by two separate routes – by X-ray reflectivity, EXAFS and electron microscopy. The EXAFS-deduced size was lower than the TEM one if a cuboctahedral fcc structural model of Pd NPs surrounded by thiol was assumed. Compared to bulk Pd, lattice expansion was noticed in all types of NPs, by both HRTEM and EXAFS.38 Regarding cobalt NPs, a report by Cheng et al. showed that EXAFS was able to differentiate ε-Co from the fcc and hcp crystal structures.39 The combination of XANES and EXAFS for the characterization of CuO, Cu_2O/CuO and CuO/TiO_2 NPs was published by Sharma et al.40 These techniques probed the local electronic/atomic structure of these samples and the existence of the different oxide phases was evidenced. Iron oxide NPs were also studied by XANES: this technique provided information on the oxidation state and local structure of iron atoms, while SAXS analysis was useful for the size determination of the particles. The combination of time-resolved in situ SAXS and XANES measurements enabled the study of the formation of maghemite NPs in water, on a structural and chemical level. On the basis of the acquired data, a complex four-stage formation mechanism was proposed, using ferrous and ferric chlorides as well as triethanolamine. The acquired knowledge would facilitate the control of the formation of NPs in solution and tailor the properties of the final product.41 In another publication, Leveneur et al. investigated the nucleation and growth of Fe NPs in SiO_2 by TEM, XPS and XANES. It was demonstrated that ion implantation initially resulted in the formation of dilute cationic Fe^{2+} species, while at higher dissolved iron concentrations, the formation of small metallic nuclei was noticed, which seed the nanocluster growth during prolonged implantation or annealing. XANES is a technique far more sensitive to coordination and bonding environment than XPS since it probes the unoccupied electronic states of atoms and therefore can provide information about the crystal field (octahedral, square pyramidal or tetrahedral) that the iron cations occupy. The complementary use of both XPS and XANES was considered to be handy for such types of nanostructures with complex compositions and various possible states for the valence of iron.42 Similar to the XRD method presented above, the SAXS technique allows elastic scattering processes into a given solid angle to be run; however the detector in SAXS covers only small scattering angles (normally lower than 1°).34 A scheme that illustrates an in situ setup which manages to record real-time SAXS/WAXS/UV–Vis measurements during the formation of Au NPs is displayed in Fig. 1. The pictured device conducts SAXS and WAXS and records the UV–Vis spectra at the same time in a given sample volume.43 WAXS (wide-angle X-ray scattering) is similar to SAXS, but the distance between the sample and the detector is smaller and therefore diffraction maxima at larger angles are observed. The authors investigated the nucleation and growth kinetics of gold NPs as a function of parameters such as concentration, temperature, ligand ratio and solvent type. Stuhn and co-workers characterized extensively polystyrene-grafted SiO2 NPs, using techniques such as SAXS, SANS, DLS, TGA and TEM. Small angle neutron scattering (SANS) provided direct access to the static structure of the polymer layer. Both SAXS and SANS can be used to measure the particle size; in that report, SAXS gave a 25.6 nm value, while a 23.3 nm NP size was derived by SANS. Although SANS and SAXS are very similar in various aspects (e.g. SANS uses elastic neutron scattering), the advantages of SANS over SAXS include its sensitivity to light elements, the possibility of isotope labelling and the strong scattering by magnetic moments.44 The ligand shells on small ZnO NPs were characterized by a combined SANS/SAXS approach. Standard in situ methods such as UV-Vis and SAXS are sensitive only to the ZnO core; however SANS probes the organic stabilizer in dispersion thanks to the high sensitivity of neutrons to H2. In the work under discussion, both techniques allowed the determination of the size distribution of the cores of the NPs and the distribution of the stabilizer molecules (acetate shell) simultaneously in the native solution.45 Fig. 1 Schematic presentation of the in situ setup employed for real-time SAXS/WAXS/UV–Vis measurements during the formation of Au NPs. The setup measures SAXS, WAXS and the UV–Vis spectra simultaneously in the same sample volume. Reprinted with permission from ref. 43. Copyright 2015 American Chemical Society. Typically, SAXS is used to determine the particle size, size distribution, and shape. Regarding size values, SAXS results are more statistically average than TEM imaging. Wang et al. employed SAXS to investigate the structural change of Pt NPs with temperature.46 For certain temperatures, the size obtained by XRD was different from the corresponding SAXS value. This is because SAXS is sensitive to the size of the fluctuation region of electronic density, but XRD is sensitive to the size of the long-range order region. SAXS provides the actual particle size, while XRD yields the crystallite size. It is important to note that the different size values of SAXS and XRD are related to the growth mode of NPs during thermal treatment. The particle size acquired with SAXS was found to be a little bigger than that obtained from TEM. The reason is that Pt NPs were coated with PVP, and the scattering intensity due to the PVP coating cannot be easily removed.46 It has to be noted that SAXS is a low resolution technique and in certain cases further studies by XRD and/or electron diffraction techniques are indispensable for the characterization of NPs. In fact, Ti et al. have written a lengthy review article dedicated to the role of SAXS for nanoparticle research.47 In the case of PVA-stabilized Ag NPs, SAXS enables a more quantitative understanding of the correlations between the localised surface plasmon resonance (LSPR) behaviour and the aggregation phenomena. Structure–property correlations between the LSPR behaviour and the SAXS spectra are feasible as both are scattering phenomena, which happen in the sol state. Moreover, the size range of the NPs which show LSPR is similar to that measured by SAXS.48 Bulavin and colleagues reported a combined approach with SAXS, UV-Vis and QELS (quasi-elastic light scattering) to characterize silver sols in polymer matrices. SAXS analysis showed a monomodal scatterer size distribution, whereas QELS and UV-Vis yielded a multimodal particle size distribution. This discrepancy might come from the ability of the latter techniques to register large particles or aggregates within the range of 30–60 nm. These large particles and aggregates are not within the detection limits of SAXS. However, for relatively small particles, all the aforementioned methods were in good agreement for the evaluation of the particle size and polydispersity.49 In the case of Ag–Cu alloy NPs synthesized using Cu- and Ag-nitrates in water with hydrazine as the reductant and starch as the sol-stabilizing agent, SAXS demonstrated the formation of mass fractal aggregates. A bimodal size distribution was noticed, with the smaller aggregates having Ag-rich compositions, while larger aggregates with low mass fractal dimensions were Cu-rich. This bimodal composition mode was also evident in the LSPR spectra. It is important to note that in view of the large scale of the NP aggregates, which is related to LSPR changes, SAXS is the most suitable non-invasive technique for these studies. In typical invasive techniques, such as TEM and SEM, the substrate–particle interactions and the solvent drying kinetics may affect the nanostructures formed. These techniques cannot thus be helpful to analyse sol structures and explain adequately their LSPR behaviour.50 In another work, Hashimoto and co-workers focused on the kinetics of the reduction-reaction-induced self-assembling process of (Pd)n in the polystyrene-block-polyisoprene (PS-b-PI) matrix by time-resolved SAXS. Pd(acac)2 was used as precursor, and it was found that its reduction to Pd(0) obeyed the first-order kinetics in both the disordered and ordered PS-b-PI matrix.51 Takenaka and co-workers performed a 'screening' of the photoreduction synthesis of rhodium and palladium NPs in aqueous ethanol/PVP solution using in situ and time-resolved SAXS. The nucleation, growth and particle coalescence of metal atoms for the production of metal NPs were monitored successfully.52 In general, SAXS helps to quantify the mass or concentration of NPs as well as their size simultaneously, as a function of time. The evolution of size, size distribution, amount and total volume of these Rh and Pd NPs was quantitatively determined by SAXS. Moreover, the formation process of mesostructured PtRu NPs electrochemically reduced on a microemulsion lyotropic liquid-crystallic template was studied by in situ XRD, SAXS and XANES.53 These techniques, together with complementary measurements by SEM, FE-TEM and EDS, facilitated the understanding of the structural evolution, starting from the metallic precursors to the subsequent atom reduction, NP formation and aggregation, and finally mesostructure formation. Several insights were acquired, for instance, the degree of alloying between both metals was studied, and any composition distribution (e.g. Pt-rich core and Ru-rich shell) was attributed to the different reduction rates of the Pt and Ru precursors. In another work, LaGrow et al. used in situ synchrotron small-angle X-ray scattering to monitor the growth and interparticle interaction of Ni NPs in solution as a function of time, and for different trioctylphosphine/Ni precursor proportions in order to understand the influence of the TOP amount on the growth kinetics. It was found that the TOP/Ni ratio affected radically the final Ni NP size because of the action of TOP as a nucleating agent, together with the fact that TOP hindered the capacity of the nickel precursor to reach the NP surface.54 Metal oxide NPs have also been investigated extensively by SAXS. In particular, grazing-incident SAXS (GISAXS) and AFM were employed to study self-assembled iron oxide NPs prepared by a high-temperature solution phase reaction, as well as silicon dots produced by ion bombardment.55 GISAXS is a unique non-destructive technique, which detects the diffusely scattered X-ray intensity from nanoscale objects (through a large illumination area), providing information on properties such as NP size, shape and arrangement. AFM can fit well with GISAXS by delivering a localized morphological image of the surface of the material. Tobler and colleagues tried to shed light on the nucleation and growth steps of SiO2 NPs, through SAXS and DLS measurements. DLS is much more sensitive to the presence of aggregates in comparison with SAXS; thus it is more suitable to monitor the starting step of the aggregation process.56 The SAXS and DLS results confirmed that the rate of silica polymerization and nanoparticle formation was enhanced by increasing the ionic strength and silica concentration. SEM and TEM verified the results obtained by SAXS and DLS regarding the particle size and shape although under certain conditions (sample dehydration, exposure to high vacuum), the microscopy techniques yielded smaller NP size compared to SAXS and DLS. Titania NPs prepared by the reaction of TiCl4 with HCl were studied by a combined approach using SAXS, DLS and TEM. While DLS provides information only on the average hydrodynamic diameter of the particles and not on their internal features, SAXS and TEM were employed to unravel such details. The authors stated the importance of SAXS for the investigation of condensed and solid matter as well as for processes in colloidal systems.57 In another work, TiO2 NPs were studied by SAXS, DSC and WAXS. The capacity of SAXS to determine the structure of a nanocomposite polymer electrolyte was noted; in the work under discussion, (PEO)8ZnCl2 polymer electrolytes and nanocomposites were doped with 10% of TiO2 nanograins and γ-irradiated.58 The effect of the inserted nanoscale titania grains on the electrical, elastic and morphological properties of the nanocomposites, and the influence of γ-radiation from a Co-60 source were investigated with the aforementioned techniques. In contrast to WAXS, which showed lines and nanocrystallites only in low temperature crystalline phases, SAXS was able to demonstrate the existence of nanograins in both the low and high temperature phases. While WAXS evidences only nanocrystallites, SAXS records the presence of both crystalline and amorphous structures. All techniques together showed that this complex material showed a transition from a crystalline–amorphous phase to a highly conductive superionic one. In another work, SiO2/TiO2 hollow NPs in the size range of 25–100 nm were studied by a combination of SAXS, GISAXS, SANS, TEM, DLS and other techniques. Experimental broadening of the scattering was negligible in the case of SAXS and GISAXS measurements, but it was not negligible in SANS.59 In general, the results for the NP size derived by all techniques were in reasonable agreement. SAXS/GISAXS provided accurate information on the inner diameter, outer diameter and size distribution. TEM sometimes overestimated the shell thickness, unless HRTEM was used. DLS was considered to be able to provide fast and cheap analysis, but SAXS was more reliable in determining polydispersity. ZnO NPs were also investigated by SAXS in various cases. More specifically, the structural evolution of zinc species toward ZnO NPs prepared with a sol–gel synthesis route using zinc oxy-acetate as the Zn source was studied by SAXS, UV-Vis and Quick-XAFS.60 The precursor led to the formation of NPs through a hydrolysis–condensation pathway in ethanol solution, induced by the addition of sodium hydroxide. ZnO/SiO2 nanocomposite thin films were investigated by GISAXS/WAXS/ellipsometry experiments. These measurements helped to evaluate the film structure (thickness, porosity, and density) as an evolution of temperature, since annealing was needed to acquire the final structure, starting with TEOS and ZnCl2 precursors.61 Post-synthetic thermal treatment improved the crystallinity of ZnO and helped the creation of oxygen-related defects from the grain boundaries, which could have radical influence on the photoluminescent behaviour. The above-mentioned measurements were also useful for the comprehension of the formation kinetics. Finally, zinc oxide NPs encapsulated into zeolite-Y were analysed through an in situ combined XRD, XAFS and SAXS approach. NaOH was employed to assist the encapsulation of zinc into the zeolite using aqueous zinc acetate as the Zn source. The particle sizes estimated by EXAFS and SAXS were in agreement with the cavity size of zeolite-Y.62 In another report, the clustering and dispersion behaviour of carboxylic acid-modified ZrO2 NPs in several solvents was evaluated by SAXS/SANS measurements. Such experiments helped to identify with precision the structural details of surface-modified NPs, including the sizes of the inorganic core and the organic shell, as well as their secondary clusters. Concerning the size measurement, the authors note that TEM provides solely the structural details in the dry form, which can differ from what occurs in the liquid state. On the other hand, DLS refers to the dispersed state, but a correct assignment of the refractive indexes for the NPs and the solvent is necessary to obtain reliable measurements. For these reasons, the authors highlighted the relatively better precision that SAXS/SANS can offer for the NP size determination.63 Tin oxide (SnO2) NPs were also investigated by SAXS: the effect of an acetylacetonate (acac) complexing ligand on the formation and growth of such particles, generated by the thermohydrolysis of SnCl4−n(acac)n at 70 °C, was analysed.64 SAXS and EXAFS were also employed to study the formation process of SnO2 NPs produced after dissolving tetrachloride pentahydrate in acid ethanol solution and subsequent heating at 70 °C.65 A five-step formation mechanism was suggested. Time-resolved SAXS experiments helped to monitor the evolution of the number and size of some intermediate species, known as nanoscopic polynuclear tin-oxo clusters. X-ray photoelectron spectroscopy (XPS) is the most widely used analytical technique for surface chemical analysis, also employed for the characterization of nanoscale materials. Its underlying physical principle is the photoelectric effect.66 XPS is a powerful quantitative technique, useful to elucidate the electronic structure, elemental composition and oxidation states of elements in a material. It can also analyse the ligand exchange interactions and surface functionalization of NPs as well as core/shell structures, and it operates under ultra-high vacuum conditions. Nag and co-workers have published a review paper describing the role of XPS as an interesting means to study the internal heterostructures of NPs. For example, it has been used to investigate the environment-dependent crystal structure tuning of metal chalcogenide NPs of various sizes.67 It can also distinguish between core/shell and homogeneous alloy structures, and identify the bonding mode of ligands such as trioctylphosphine oxide (TOPO) onto the surface of metal chalcogenide NPs. For example, if TOPO bonds preferentially to the surface metal element, then the uncapped surface chalcogenide element may oxidize more easily upon exposure to air. In comparison with microscopy techniques, like TEM and TEM/EELS, which use lateral spatial resolution to identify elements in a direction vertical to the probing electron beam, XPS probes the composition of the material along the direction of the electron beam. Regarding core–shell NPs, Shard has published an article that reports a straightforward method to interpret the XPS data for such types of particles. It involves a direct and accurate empirical method to convert the XPS intensities into overlayer thicknesses, mostly suitable for spherical NPs.68 As further advantages of XPS the author mentions that it provides the depth information, similar to the size of NPs (up to 10 nm depth from the surface) and it does not significantly damage the samples. Two drawbacks of XPS analysis are the preparation of samples (i.e. dry solid form is required without contamination) and the interpretation of data. In another study, the interaction of L-cysteine with naked Au NPs has been studied with XPS: that report aimed to provide experimental spectroscopic support to the kinetic models of catalyst deactivation, studying the role of low-coordinated Au atoms belonging to NP edges and corners.69 Furthermore, Minelli and co-workers wrote an article on the analysis of protein coatings on Au NPs by XPS and liquid-based particle sizing techniques. XPS is robust and useful to study proteins quantitatively, as well as peptides adsorbed at Au interfaces. It can also characterize the molecular interface of Au NPs. The chemical information from the NP surface analysed by XPS can be used to assess the thickness of NP coatings.70 Smirnov et al. used the so-called Davis' method to determine the size of Au NPs in the planar model Au/C systems based on the data of XPS. The NP size values derived by XPS agreed well with those from the scanning tunneling microscope (STM) data, with the degree of similarity being related to the particle shape (e.g. sphere, hemisphere and truncated hemisphere).71 Tunc et al. presented a simple method by applying an external voltage stress during the XPS analysis of Au@SiO2 NPs; their method facilitated the detection, location and identification of charges developed on surface structures in a completely non-contact mode. Therefore, XPS provided information not only on the chemical identity but also on the dielectric properties of nanomaterials, by recording their charging/discharging behaviour.72 In another work, Polzonetti and colleagues used synchrotron XPS and NEXAFS to study the interaction at the molecule–metal interface and ligand arrangement in the molecular shell of Au NPs capped by aromatic thiols. The experimental results of both techniques were supported by density functional theory (DFT) calculations, illustrating the presence of a hybrid system in which the metallic Au core was surrounded by a shell of aromatic thiol molecules, whose thickness could be assessed by XPS.73 Castner and co-workers quantified the impact of nanoparticle coatings and non-uniformities on XPS analysis, for the case of Au@Ag core–shell NPs. They analysed the benefits of a complementary approach using XPS, STEM and simulated electron spectra for surface analysis (SESSA) simulations to characterize the structure and composition of NPs with nonideal geometries.74 For instance, STEM provided information concerning the metallic cores and shells, while XPS provided information regarding organic species and contaminants that were difficult to identify by STEM.74 In another report, Ag NPs capped with taurine were investigated by SERS and XPS. The latter method together with DFT calculations showed that the quencher of taurine was the main component of the Ag surface.75 XPS confirmed the binding of taurine through the oxygen atoms of the sulphonate group, denoting the existence of 71% Ag(0) in taurine-functionalized Ag NPs. This protocol provided a quantitative understanding of the interaction of the above molecule with Ag NPs. Furthermore, Ramstedt and Franklyn produced Ag NPs inside a poly(3-sulfopropyl methacrylate) brush and studied their formation process with TEM, UV-Vis and XPS. The apparent oxidation state of Ag in the different forms (NPs, films, and clusters) was investigated using XPS and a chemical state plot.76 In the case of bimetallic Ag/Pt colloids, prepared by galvanic replacement onto Ag colloids pre-synthesized by laser ablation, the final product was investigated by UV-Vis, XPS, SERS and Z-potential.77 Nevertheless, it was not easy to distinguish between Ag(0) and Ag(I) through XPS analysis. The galvanic replacement process was monitored by the Z-potential measurements on the basis of the fact that the charged species on the Ag surface had a progressively modified adsorption due to the oxidative action of air diluted in an aqueous medium. CdS@Ag2S core/shell NPs prepared with the AOT/n-heptane/water microemulsion technique were characterized by XPS and SEM-EDX (EDS stands for energy-dispersive X-ray spectroscopy).78 The authors emphasize the benefit of XPS in comparison with SEM-EDX as the photoelectron energy and the respective binding energy are characteristic of each element. The intensity of the peaks is a function of the concentration of the respective element. The XPS and SEM-EDX results supported the core–shell formation. In another work, Ag, Ni, and AgNi NPs synthesized by the seed-mediated growth method on a transparent conductive indium tin oxide substrate were studied by XPS, XRD and optical spectroscopy. XPS determined the oxidation states of Ag and Ni at the outer layers of the NPs. It was shown that the surface of Ag NPs was not oxidized, while Ni NPs were oxidized to nickel oxide and hydroxide.79 It is interesting to note that no peaks of NiO or Ni(OH)2 were detected in the XPS spectrum of the bimetallic AgNi NPs; for AgNi, silver in Ag(0) state and oxidized Ni atoms were detected. This indicated the presence of a Ag core@NiO–Ni(OH)2 shell structure. Kalinkin et al. investigated the oxidation of small Pt NPs on graphite with NO2, using XPS and STM. The combination of these techniques provided information on the state and structure of the surface of the NPs and could facilitate the understanding of the origin of the size effect.80 In fact, only Pt NPs with a size smaller than 2.5 nm were found to oxidize to a mixture of PtO and PtO2 under the experimental conditions of that study. Chakroune et al. studied acetate- and thiol-coated Fe NPs with XPS, SAS and HRTEM. For Fe stored in polyol, surface oxidation limited to one monolayer and a surface coating with mainly acetate ions were evidenced by XPS measurements.81 For particles capped with thiol after being prepared in polyol, the formation of a Fe–S bond was shown for very small (2 nm) ruthenium particles. XANES and XPS were in agreement with charge transfer from Ru to S atoms. Rhodium NPs, prepared by reducing RhCl3·3H2O in a water/ethanol/PVP mixture, were characterized by several techniques, including XPS and NEXAFS. These techniques investigated the chemical states and indicated that the chlorine moiety derived from the precursor remained at the obtained NPs at both surface and bulk volume but heating may have caused its removal.82 In another work, Ir NPs were produced by decomposing [Ir(COD)Cl]2 in dichloromethane in the presence of an ionic liquid under a hydrogen atmosphere. XPS helped to identify the interaction of Ir(0) NP surface with ionic species of the imidazolium ionic liquid 1-ethyl-3-methylimidazolium ethylsulfate (EMI·EtSO4).83 Zerovalent Fe NPs were applied by Li and Zhang for the removal of water contaminants, such as Cd(II), Pb(II), etc. HR-XPS confirmed that these Fe NPs had a core–shell structure, which resulted in remarkable properties for concurrent sorption and reductive precipitation of metal ions. Such measurements facilitated the identification of the type of element present at the NP surface, the chemical and valence states of these elements and the ratio between the different chemical states of each element. These core/shell Fe/Fe oxide NPs were highly efficient in metal removal.84 Moreover, Sheng et al. used zerovalent Fe NPs immobilized onto diatomite for the sequestration of uranyl (U(VI)) in water. The XPS experiments implied that the diatomite-supported Fe NPs helped to reduce the highly toxic and mobile UO22+ to less toxic and mobile UO2.85 Complementary characterization with EXAFS illustrated that diatomite could act as a scavenger for insoluble products like Fe(III), therefore enabling more reactive sites to be used for (U(VI)) reduction. The utility of XPS to acquire information of ligand binding on NPs coated with several types of ligands was demonstrated by Lee and co-workers. The particles studied were CdSe/ZnS quantum dots capped with TOPO, 3-mercaptopropionic acid (MPA) or 1H,1H,2H,2H-perfluorooctanethiol (PFOT). Their analysis with XPS imaging had low sensitivity and limited lateral resolution; however, it provided a statistical, non-destructive method to characterize the ligand–QD binding mode.86 In addition, near ambient pressure (NAP)-XPS was employed to record the oxidation state of palladium in PdO NPs supported on TiO2 at a temperature range of 30–120 °C. PdO was used to catalyze the oxidation of 2-propanol. Lab-based NAP-XPS instead of synchrotron facilities showed distinct advantages: the instrument is available upon need and it can be integrated permanently with other devices for optimal sample analysis, but there are also some disadvantages: a synchrotron source results in photoelectron peaks with higher intensity, thus obtaining measurements at a higher resolution. However, care needs to be taken because a high-intensity radiation source can destroy certain types of samples. Overall, NAP-XPS is an effective technique to study in situ the steady-state conditions at the solid–gas interface, which are significant in the domains of catalysis, electrochemistry, corrosion and environmental science. The authors mention that additional screening with techniques such as mass spectrometry was needed for a more complete picture of the catalytic process (oxidation of 2-propanol by PdO NPs in this case) in such reactions.87

2.2 Additional techniques for the characterization of the structure, composition and other main NP properties

There are also several other techniques that help in the determination of the structure, composition, size and other basic features of the NPs. Fourier transform infrared spectroscopy (FTIR) is a technique based on the measurement of the absorption of electromagnetic radiation with wavelengths within the mid-infrared region (4000–400 cm−1). If a molecule absorbs IR radiation, the dipole moment is modified and the molecule becomes IR active. A recorded spectrum gives the position of bands related to the strength and nature of bonds, and specific functional groups, providing thus information concerning molecular structures and interactions.88 Fellio and co-workers studied how Pt nanostructures performed on ethanol oxidation, using a combined approach with in situ ATR-FTIR and differential electrochemical mass spectroscopy (DEMS). These techniques helped to probe adsorbates electrochemically and detect volatile reaction products. Their results were in agreement with previous findings, showing that the preferred decomposition products were related to surface structures, with COads formation on (110) domains and acetaldehyde/acetic acid formation on (111) domains.89 In another report, carbon-supported platinum NPs (3–8 nm size) were used for the CO oxidation reaction and this catalytic process was monitored using DRIFTS and quadrupole mass spectrometry (QMS). The FTIR measurements of adsorbed CO confirmed the variations of COad and Oad in different steps of the experiment, in accordance with the results from QMS, while modifications in the CO stretching over various types of Pt surface sites were also noticed. Overall, DRIFTS was regarded as an important tool for the probation of the surface structure of Pt NPs under in situ conditions.90 Shukla et al. published a paper devoted to the FTIR investigation of the surfactant bonding to FePt NPs that were synthesized in the presence of oleic acid and oleylamine. The former ligand was found to bond to FePt NPs in both monodentate and bidentate forms, while oleylamine bonded to FePt molecularly with the NH2 group intact.91 Furthermore, Au/Ag bimetallic NPs stabilized with dodecanethiol and soluble in nonpolar solvents were produced through a two-phase synthetic route in water/toluene mixtures.92 The most important aspect in this report was the use of FTIR, which helped to determine that Ag atoms were enriched at the outer part of the alloy clusters in comparison with the Au atoms. In another work, the influence of the Ag NP content on the photocatalytic degradation of oxalic acid adsorbed on TiO2 NPs was evaluated by ATR-FTIR. Various Ag NP amounts were tested, and it was demonstrated that the incorporation of only a small quantity (2%) boosted the photocatalytic performance of TiO2 NPs substantially. AFM and XPS were also employed to characterize the topography and chemical structure/composition of the composite NP films.93 Tzitzios et al. synthesized Ni NPs with a hexagonal crystal structure in the size range of 13–25 nm via the reduction of nickel stearate in the presence of PEG, oleic acid and oleylamine. FTIR spectra showed the presence of the characteristic groups at the surface of the NPs, such as the –HCOH– arrangement in OAc and OAm, while the binding modes of the ligands onto the NP surface were also examined.94 Copper zinc tin sulpho-selenide (CZTSxSe1−x) nanocrystals were prepared by Haram and colleagues with a hot-injection process. The precursors were dissolved in OAm and heated at T = 200 °C for the synthesis. FTIR measurements showed the adsorption of OAm onto the surface of the particles. Characteristic bands arising from the moieties existing at the molecule of OAm and indicating its successful coordination with the NPs were spotted.95 Superparamagnetic ferrite NPs (MFe2O4, M = Ni, Co, Zn, Mn) with high crystallinity and size below 10 nm were synthesized by Sabale et al. with a simple 'polyol' method. The observation of tetrahedral (ν1) frequency at the FTIR spectrum verified the formation of the spinel ferrite structure. Bands assigned to the –OH and C–O groups denoted the presence of diethylene glycol, thus revealing its successful coating around the ferrite NPs, endowing them a high solubility in water.96 In another report, the presence of P–O–P bonds was shown by FTIR measurements for hydrophobic iron nanoparticles which were treated with alkyl phosphonic acid-based ligands in order to turn them into water-soluble iron-oxide core–shell NPs.97 FTIR spectroscopy was also employed to characterize the multifunctional Fe3O4@C@Ag hybrid NPs, which were prepared with a facile route based on the direct adsorption and spontaneous reduction of Ag ions onto the surface shell of C-coated magnetic NPs. The presence of carboxyl and hydroxyl groups on the NP surface was proven by FTIR, whereas the reduction of Ag ions, which was enabled by the carbonyl and hydroxyl groups, was also exhibited. These hybrid NPs displayed a remarkable photocatalytic activity for the photodegradation of neutral red dye under visible light irradiation.98 FTIR was also used to study the attachment of ligands on the surface of NaYF4:Yb/Er upconversion nanoparticles.99 Triethylphosphine-stabilized CdS nanorods synthesized by Chen et al. were also characterized by FTIR, revealing C–P stretching peaks related to the aforementioned molecule.100 Table 3 presents the IR vibrational assignments of several characteristic functional groups which are involved in nanoparticle synthesis.101

Table 3 Selected infrared vibrational assignments for some of the most common groups present on the surface of NPs101

Vibrational modes	Frequency (cm−1)
Methyl C–H asym/sym stretch	2970–2950/2880–2860
Methyl C–H asym/sym bend	1470–1430/1380–1370
C=C alkenyl stretch	1680–1620
Aromatic C–H stretch	3130–3070
O–H hydroxyl group, H-bonded OH stretch	3570–3200 (broad)
C–O stretch, primary alcohol	~1050
N–H aliphatic primary amine, NH stretch	3400–3380, 3345–3325
N–H primary amine, NH bend	1650–1590
C–N, primary amine, CN stretch	1090–1020
Organic phosphates (P=O stretch)	1350–1250
Aliphatic phosphates (P–O–C stretch)	1050–990
Sulfonates	1365–1340/1200–1100
Organic siloxane or silicone (Si–O–Si)	1095–1075/1055–1020
Organic siloxane or silicone (Si–O–C)	1100–1080
Thiols (S–H stretch)	2600–2550
Thiol or thioether, CH2–S– (C–S stretch)	710–685
Aliphatic chloro-compounds, C–Cl stretch	800–700
Ammonium ion	3300–3030/1430–1390

Nuclear magnetic resonance (NMR) spectroscopy is another important analytical technique in the quantitative and structural determination of nanoscale materials. It is based on the NMR phenomenon exhibited by nuclei that possess non-zero spin when placed in a strong magnetic field, which causes a small energy difference between the 'spin-up' and 'spin-down' states. Transitions between these states can be probed by electromagnetic radiation in the radio wave range. NMR is typically used to study the interactions or coordination between the ligand and the surface of diamagnetic or antiferromagnetic NPs. It is, however, not suitable to characterize ferri- or ferromagnetic materials, as the high magnetic field leads to shifts of the signal frequency and dramatic decreases in relaxation times. As a result, significant broadening of the signal peaks occurs, making the measurements practically insensible and unable to be interpreted.66 Marbella and Millstone have written a comprehensive review article on the NMR techniques for noble metal NPs. NMR spectroscopy can help toward the routine, straightforward, molecular-scale investigation of NP formation and morphology in situ, in both solution and solid phase. It is particularly useful for analysing both the formation and final architecture of noble metal NPs. The capping ligands are also typically studied by NMR, and such measurements can yield information on the properties of the particle core (e.g. electronic structure, atomic composition, or compositional architecture). Insights into ligand density, arrangement and dynamics can also be derived.102 Besides facilitating the monitoring of the chemical evolution of ligand precursors and their role in particle growth, NMR is also employed to probe the role of capping ligands for the determination of particle shape. Overall, NMR can screen the chemical transformation of NP precursors in both the solution and solid phase, with high spatial and chemical resolution, under distinct reaction conditions, and for diverse metal identities; this helps in the better comprehension of the reaction mechanisms for NP synthesis. For instance, NMR is useful for the monitoring of the process and final products of ligand exchange, when the initial capping ligands need to be replaced.102 The 1H NMR chemical shift behaviour is sensitive to the surrounding electronic environment; this includes the electronic structures and bonding environment of the nucleus. Consequently, any changes in the handedness of a molecule can be 'felt' by neighbouring spin positions and observed as changes in chemical shift. This renders NMR significant to assess the chirality or absence of chirality of small molecule-like nanoclusters. NMR can also be applied for the direct monitoring of the diffusion of adsorbed gases onto the surface of metal NPs. Finally, NMR is utile for the measurement of the hydrodynamic radius of metal NPs and thus constitutes an important complement to more standard NP sizing techniques, such as TEM and DLS. Similar to DLS, NMR spectra are used to define the NP size via the analysis of diffusion. In particular, NMR helps to extract the diffusion coefficient of well-dispersed species in solution diffusing according to Brownian motion only. Then the hydrodynamic size can be calculated through a rearrangement of the Stokes–Einstein equation.102 Finally, a phenomenon known as 'Knight shift', which is induced by the electron density, can be present upon NMR measurements, as is described in ref. 102. It has to be noted that the particle size, which can be safely analysed by NMR, can exceed by far the 100 nm in the case of polymer-hybrid particles,103,104 whereas metallic NPs have to be at around the size range of 1–5 nm in order to acquire meaningful NMR measurements. 1H solution NMR has been reviewed by Hens and Martins as a tool for the investigation of the surface chemistry of colloidal NCs.105 Diffusion-ordered NMR (DOSY NMR) offers the possibility to distinguish in situ free ligands from bound ligands, while the distribution of these species can also be quantified. Solution NMR can be employed to identify tightly bound ligands and quantify their surface density of sterically stabilized colloidal NPs.105 Jeczusky and co-workers studied hydrophilic heptakis(6-deoxy-6-thio)cyclomaltoheptaose capped Au NPs by NMR spectroscopy. This proved to be an effective, reliable and rapid way to investigate the role of the local concentration of gold in the solid mixed atom (SMA) solutions as well as of the Au/ligand molar ratio on NP sizes. NMR spectroscopy also helped to acquire some basic information on the drug transport and release capabilities of Au NPs. This was achieved through the analysis of the nature of supramolecular aggregation processes and the ability of (Au)n-β-CDSH nanoaggregates to act as hosts for doxycycline (DX).106 DOSY-NMR was also employed to characterize the coating of Au NPs prepared by Canzi et al. This was achieved by analysing the 1H spectrum of the protecting ligands using 2D DOSY NMR, a method that could be facilely adapted also for other metal and semiconductor nanocrystals. Size estimates were acquired by using diffusion coefficient ratios derived from the proton signals from the alkyl thiolate groups bound to Au NPs and a ferrocene internal standard. The authors noted that DOSY NMR was a reliable alternative method to calculate the NP size, being quicker and more cost-effective than TEM.107 Coelho and colleagues used NMR spectroscopy to determine particular intermolecular interactions and mechanisms of drug immobilization and location onto surface PEG-modified Au NPs. The authors highlighted the advantages of NMR as a non-destructive, highly reproducible method, sensitive to the structural changes of both NPs and molecular conjugates, which could be applied for both qualitative and quantitative characterization. Information of size, shape, dynamics, chemical structure, intermolecular interactions, and binding and exchange processes in complex nano-systems could be obtained.108 The combined use of NMR with FTIR, UV-Vis, DLS and TEM could yield significant insights regarding important physicochemical properties of drug delivery systems, which influence their therapeutic efficacy.108 In another report, deuterium (2H) NMR was employed to study the (d15-PPh3)-capped Au NPs. The authors made use of the ability of NMR to probe ligand structure and surface binding properties on NPs by the in situ analysis of chemical shifts and resonance lines in the solid and liquid states. A specific feature of 2H NMR is its simplicity and the capacity to distinguish the type of dynamics in amorphous and crystalline domains, for organic compounds that are isotopically labelled with deuterons.109 Smith et al. used NMR to investigate the extent of ligand exchange between distinct kinds of thiolated molecules on the surface of Au NPs. In particular, they obtained spectra for single-moiety ligand shells and then used these data to describe the ligand exchange behaviour with a second, thiolated molecule.110 Triphenylphosphine-capped 1.8 nm Au NPs have been characterized by multinuclear NMR to investigate their surface structure and ligand binding environment. In solution, the ligand exchange kinetic reactions were screened by 1H, 2H and 31P NMR to analyse the ligand exchange process.111 Doyen et al. used UV-Vis and NMR to study the formation of Au NPs by the citrate reduction method. 1D-1H and DOSY-NMR measurements showed that citrate aggregates with Au(I) and Au(0) were formed. That work suggested that citrate, apart from being the reductant and the stabilizing agent for Au NPs, might act as a 'molecular linker', which could help in the particle formation.112 The coordination of amine ligands on Ag NPs was studied by NMR, SERS and DFT.113 It was found by SERS that the amidine moiety, coming from the silver amidinate precursor, remained bound to the metal surface, whereas the hexadecylamine ligand was in a fast exchange between a surface-bound state and free floating in solution, as revealed by NMR. Solution NMR spectroscopy was a powerful tool for the analysis of short timescale effects. Long-residence-time molecules at the NP surface could not be monitored by this technique due to their very slow tumbling. The SERS analysis of the NPs combined with DFT modelling demonstrated that unexpected organic groups were observed by this latter technique, in contrast with what was shown by solution NMR. SERS is efficient if molecules are in a close contact with the Ag surface, whereas NMR spectroscopy examines molecules in the first and second coordination sphere of the NPs. Despite this, the complementarity of SERS with NMR is beneficial to reveal the molecular environment of the prepared NPs. Amidine hindered the NP aggregation, while hexadecylamine (HDA) helped toward a narrow size distribution of stabilized Ag0 NPs.113 Ag NP/π-conjugated polyelectrolyte systems were investigated by NMR, FTIR and SERS and increased regularity of the high-cis polymers was documented. The IR spectra supported the conclusions drawn from the 1H NMR measurement of the polymer; both techniques consistently illustrated the cis-rich configuration of polymers formed by the solution polymerization in acetonitrile and the cis/trans configuration of the polymers formed by the bulk polymerization.114 Velders and co-workers focused on the use of 1H NMR spectroscopy to determine the NP size in the case of dendrimer-encapsulated Pd NPs. The advantage of NMR in comparison with TEM consisted of its capacity to probe the total population of the NPs, providing more representative information regarding the average NP size. In addition, in situ operation was possible with NMR, and this enabled the monitoring of the changes in the size and the capping ligand environment of the NPs during catalytic reactions.115 Solution NMR spectroscopy has been extensively used also for the characterization of oxide nanoparticle systems. Kahn and co-workers characterized ZnO NPs by 1H and DOSY-NMR. They emphasized on the ability of the latter technique to sort species according to their size, as the diffusion coefficient is inversely proportional to the hydrodynamic radius. Their study, performed on ZnO NPs stabilized by amine molecules, showed that a fast exchange between free and coordinated amine molecules was deduced within the NMR measurement timescale. Overall, the NMR spectra showed that the seemingly simple stabilization of ZnO NPs by amine molecules appeared to be much more complicated than considered beforehand.116 The same group published a study dedicated to the use of NMR techniques for the investigation of the role of amine ligands together with oleic acid on the formation of ZnO NP superlattices in C7D8. Their experiments demonstrated the dependence of the type of ligand adsorbed on the NP surface on the concentration of the colloidal NP solutions. It was suggested that the driving force of the superlattice formation was the presence of ion-paired ammonium carboxylate shells around each particle.117 Yarger and colleagues investigated phosphonic acid-capped SnO2 NPs with sizes lower than 5 nm, using multinuclear solution and solid-state magic angle spinning (MAS) NMR. The latter technique indicated the absence of acidic protons of the phosphonic acid groups, strongly supporting the formation of P–O–Sn linkages. Insights into the ligand structure and the extent of phosphonic acid protonation upon binding the NP surface were obtained.118 In the case of Ca2SnO4 NPs prepared by the mechanochemical synthetic route, 119Sn MAS-NMR and 119Sn Mössbauer were employed to probe the local environment of Sn nuclei, so as to acquire important insights into the local structural disorder of these NPs. NMR spectroscopy provided information on the magnetic and chemical interactions, while Mössbauer measurements revealed the quadrupolar interactions experienced by the nuclei of 119Sn.119 Magnetite-silica NPs prepared by a two-stage procedure by Bogachev et al. were characterized by NMR relaxometry, AFM and UV-Vis spectroscopy. The aggregation process in the colloidal solutions of Fe3O4–SiO2 NPs was investigated.120 Dextran-coated γ-Fe2O3 NPs were studied by Papavassiliou and colleagues with 57Fe NMR, Mössbauer, TEM and magnetization measurements. The low temperature mechanism of collective magnetic excitation in magnetic NPs, which originated from the fluctuations of the magnetization direction around an energy minimum corresponding to an easy direction of magnetization, was investigated. 10 nm nano-sized samples at low T displayed similar NMR spectra, and thus similar hyperfine fields to the bulk material, implying that the samples had the same magnetic structure.121 Gossuin et al. characterized gadolinium hydroxide and dysprosium oxide NPs using XRD, magnetometry and NMR relaxometry. Nuclear magnetic relaxation dispersion profile represented the evolution of the longitudinal relaxation rate with respect to the magnetic field and provided interesting information about the longitudinal relaxation mechanism.122 Finally, HfO2 and ZrO2 NPs synthesized using the Karlsruhe microwave-plasma process were characterized by several techniques such as 1H MAS NMR, XPS, XRD and electron diffraction. Among these techniques, NMR and XPS helped to identify the chemical composition of the as-prepared NPs. A hydrate surface layer with a hydrogen content of 5–10 wt%, composed of chemisorbed hydroxyl groups and organic precursor fragments, was detected by 1H-MAS NMR.123 Solid-state NMR (SS NMR) spectroscopy is an important characterization tool to investigate the behaviour of solid catalysts and chemical processes occurring at their surface. Such technique may help to resolve not only interactions at the ligand–solvent interface but also result in the acquisition of significant insight into ligand–particle bonding at the hard–soft matter interface.102 For example, 31P is a very sensitive NMR nucleus with 100% natural abundance and high gyromagnetic ratio and it is quite easy to measure the 31P NMR spectra with a good signal to noise ratio even in systems with low ligand concentrations. J-resolved 31P solid-state NMR spectroscopy combined with DFT calculations can provide important information about the structure of heterogenized species and also provide insights into the immobilization of homogeneous metal phosphine catalysts. Gutmann and co-workers have highlighted the crucial role of liquid and partly solid-state NMR techniques for the detection of surface molecules and the discrimination between different binding sites on nanoscale catalysts.124 In particular, 2H MAS NMR has been employed to study chemical reactions such as the hydrogenation of olefins, being capable of detecting reactive intermediates. The authors denoted a weakness of the NMR measurements, which was related to their sensitivity. Solid state 31P NMR was used to characterize phosphinine-stabilised Au NPs and a phosphinine–Au complex, as reported by Mallissery and Gudat.125 NMR spectra showed that in addition to metal-bound intact phosphinine units, several surface-bound species generated by the chemical transformation of the initially supplied ligands were also detected. In another work, two different tripeptides attached on Au NPs were analysed by SS NMR and DFT calculations. Substantial structural differences between CysAlaAla and AlaAlaCys on Au NPs were evidenced through the aforementioned techniques. In particular, the location of the carboxylate moiety relative to the S atom that served to anchor the peptide to the surface played a significant role in determining these structures.126 Novio et al. have used SS NMR and FTIR to characterize the location and dynamics of carbon monoxide coordination on Ru NPs. Two different sets of 2 nm Ru NPs were tested, prepared under a H2 atmosphere, stabilized by either PVP or a bidentate phosphine ligand (dppb). It was demonstrated that CO groups were mobile on the NP surface, while the bulky ancillary ligand dppb slowed down the fluxionality of CO and prevented the exchange at certain positions.127 SS NMR was also employed to characterize 1–2 nm Ru NPs capped by either 1,3,5-triaza-7-phosphaadamantane or PPh3 ligands and exposed to a CO gas atmosphere. That paper presented a new way to analyse interactions and calculate approximate distances between phosphine ligands and CO probe molecules on the surface of Ru NPs employing 31P–13C REDOR NMR.128 Lara et al. decomposed [Ru(COD)(COT)] [(1,5-cyclooctadiene)(1,3,5-cyclooctatriene)ruthenium] and [Pt(CH3)2(COD)] [dimethyl(1,5-cyclooctadiene)platinum(II)] organometallic complexes to produce small core–shell RuPt NPs in the presence of PVP at room temperature. Several characterization techniques were combined for determining the structural composition of the particles, and 13CO was used for adsorption as a probe molecule. FTIR and SS NMR results were in agreement with the coordination of CO to Pt and in this way the presence of a segregated Ru core/Pt shell structure was indicated. Measurements by WAXS, HRTEM, EXAFS and other techniques corroborated these findings.129 Electrically conductive Al-doped ZnO NPs prepared by Avadhut et al. were characterized by SS NMR spectroscopy: a core–shell structure model was proposed for these NPs, which were synthesized with a microwave-assisted polyol method. A combination of different 1D 27Al, 1H, 13C and 2d 27Al{1H} SS NMR techniques helped to gain insight into the particle structure and explain the macroscopically observed conductivities as a function of the NP composition.130 Nanoscale fluorine-doped SnO2 NPs, prepared with a microwave assisted polyol approach were studied by several techniques, including SS NMR. Sn(II) could be distinguished from Sn(IV) using NMR, similar to what Mössbauer spectroscopy can do. Heteronuclear NMR experiments helped to characterize intraparticle interfaces in polycrystalline NPs. The fluorine doped particles showed an increased conductivity, after annealing, in comparison with undoped SnO2 NPs.131 Davidowski and Holland employed SS NMR to characterize mixed phosphonic acid ligand binding and organization on SiO2 NPs. Multinuclear (1H, 29Si, 31P) and multidimensional solid-state NMR techniques were used, while the phosphonic capping ligands were methylphosphonic acid and phenylphosphonic acid. For instance, 31P NMR spectra showed that phosphonic acid functionalized silica NPs displayed three different ligand environments, attributed to physisorbed, monodentate and bi/tridentate.132 The combination of multinuclear SS NMR and DFT calculations has been employed to investigate the structure of NaYF upconverting NPs. A detailed analysis of the crystal lattice and ionic distribution was achieved by these techniques. In particular, 89Y NMR was employed to probe the chemical environment of Y3+ ions in the NaYF4 structure. The presence of a solid solution type cubic structure in which cation sites were randomly occupied was observed.133 Finally, for the characterization of surface species and substrate–surface interactions on metal NPs, the groups of Pruski and Emsley have shown that dynamic nuclear polarization surface enhanced NMR can be a very useful tool for the further increase of the sensitivity of SS NMR.134,135 The Brunauer–Emmett–Teller (BET) technique is also used for the characterisation of nanoscale materials. It is based on the principle of physical adsorption of a gas on a solid surface, and it was named by the initials of the surnames of its developers, Brunauer, Emmett and Teller. It is widely used for the determination of the surface area of nanostructures, being a relatively accurate, rapid and simple method for this purpose.66 Sahoo and co-workers prepared biocompatible ferrofluid containing dye-functionalized Fe3O4 NPs, which can serve as fluorescent markers. Several techniques were used for the characterisation including BET, FTIR and others. The surface area measured by BET was smaller than the estimate obtained from the size distribution and density values of the studied material; this deviation might be caused by the agglomeration of smaller NPs resulting in larger ones, thereby effectively reducing the collective surface area. Such agglomeration risk is probably aggravated considering that the NP samples need to be dried for such measurements: strong hydrogen bonding might occur among the NP surfaces, thus, inducing a certain error.136 In another work, mesoporous polymer microspheres with Au NPs inside their pores were produced, to observe the adsorption behaviour of these NPs, considering their surface functionality and porosity. BET experiments of Au/poly(ethylene glycol dimethacrylate-co-acrylonitrile) composite microspheres, used to measure the microsphere porosity, revealed that the adsorption of Au NPs into the pores kept the pore structure intact and turned it more porous.137 Ma et al. synthesized Fe3O4 NPs by the co-precipitation method of ferrous and ferric species, resulting in a product with high specific surface area (286.9 m2 g−1). This value was much higher than those already reported in the literature for such particles.138 Thermal gravimetric analysis (TGA). While FTIR offers information about the NP–stabiliser interaction and confirmation of the stabiliser type, it does not provide insights into the extent of surface coverage or the mass to mass ratio of NP to stabiliser, which is important to normalize the values of saturation magnetization to purely metallic content, for instance. TGA provides information concerning the mass and composition of the stabilisers. With this technique, a nanomaterial sample is heated and components with different degradation temperatures decompose and vaporise, and a change of mass is recorded. The temperature and the loss of mass are recorded by the TGA device and, taking into account the starting sample mass, the type and quantity of NP organic ligands are determined.139 A method known as microthermogravimetric analysis (μ-TGA) uses the same thermal decomposition principle as TGA, but the mass of the sample investigated is in the order of 1 μg, with mass changes lower than 1 nanogram being able to be detected. In this way, the detection limits of conventional TGA can be improved to a significant extent. Mansfield et al. used μ-TGA to identify the presence and quantity of surface-bound ligand coverage on Au NPs and verify the existence of PEG coating on silica NPs.140 Their results demonstrated that the aforementioned technique is a valid one to determine quantitatively the NPs coatings, while information on the purity and compositional data of the NPs can also be acquired sometimes. The authors highlighted the advantages of TGA, which is a simple and direct technique without any special need for sample preparation, apart from having the sample in dry state. A drawback of conventional TGA is the need to have a few milligrams of the nanomaterial sample, which may raise the cost or lab-scale production feasibility issues. These researchers used a variety of NP systems to illustrate the utility and limitations of μ-TGA and its comparison with conventional TGA. For example, similar results of both techniques were obtained concerning the oxidation temperature and the residual mass measurements in carbon nanotubes. In addition, the ability to identify layer-by-layer coatings on a Au NP core was evidenced by both techniques. The same research group analysed the surface density of PEG on Au NPs by using μ-TGA. The speed and reliability of TGA to determine the fractions of thermally stable and unstable masses of a sample were exploited. Usually, the surface coverage for inorganic particles with combustible ligands can be calculated if particle size and ligand molecular weights are well known. The authors measured the PEG surface densities on Au NPs using both μ-TGA and fluorescence spectroscopy. The lower values for surface densities determined from the latter technique might be attributed to incomplete displacement of the ligands from the Au surfaces.141 In another report, thiol-terminated PEG-coated Au NPs in aqueous solution were studied by TGA and other techniques, aiming to elucidate their structure and hydration. Combining mass density, SANS, SAXS and TGA resulted in the acquisition of precise information on the Au core size and on the capping polymer chains. SANS fits reached their optimal minimizations with a three shell model: the inner one related to the Au core, while the other two are characterized by different polymer–water mixtures with distinct scattering densities. On the other hand, SAXS was principally sensitive to the dimension of the Au core, considering that the contrast in the electron densities between the polymer and the solvent is low. The results of the structural data of the scattering experiments and the volumetric data derived from mass density and TGA measurements were consistent, revealing the complementarity and correctness of this overall characterization approach.142 Jia et al. prepared Au and Pd NPs via a surfactant-free single phase solution route. High-temperature TGA coupled with mass spectroscopy (MS) was used to find the relative amounts of ionic contaminants, since protecting thiolate groups and inorganic contaminants were removed in separate weight loss events. TGA-MS helped to achieve a more accurate determination of the thiolate to Au ratios, revealing a complex composition of the NPs presented therein. TGA-MS could also distinguish between the evaporation of the original thiolate ligands and their oxidized species. The limitations of the above technique include the fact that non-volatile compounds such as Li2O cannot be detected; however, XPS, FTIR and XRD can help toward such detection. In addition, the quantification of the content of certain groups and compounds based on TGA is only precise if their weight losses take place at distinct temperatures. Events that happen at similar temperatures can be separated by optimizing the heating program. However, overlapping events may be identified by MS, but the quantification of the intensities recorded in the MS data is not simple.143 Magnetite NPs with fatty acid (ricinoleic) adsorbed on their surface were investigated with a TGA device coupled with FTIR. The decomposition of ricinoleic acid was studied by TGA under an inert atmosphere, while gas phase FTIR helped to gain information on the decomposition gases released. The impact of the autoxidation of the fatty acids was presented, while an extended reduction of magnetite from carbonaceous residues was also noticed.144 Slight discrepancies between the results from the TGA and XRD experiments on the exact composition of the iron oxides might originate from the formation of oxidized residues in these two different measurements. In another work, Nava-Etzana and co-workers reported the synthesis of BiFeO3 nanostructures by a combustion reaction, in the presence of tartaric acid or glycine as the promoter. The origin of a high purity BiFeO3 nanomaterial together with the formation of certain by-products was discussed on the basis of metal–ligand interactions. Such high product purity demonstrated by XRD analysis was corroborated with the results from TGA.145 Furthermore, TGA/FTIR and a combination of TG–gas chromatography–mass spectrometry (TG/GC-MS) were employed to characterize the effect of different types of dopants (e.g. SiO2 NPs, multi-walled carbon nanotubes, and montmorillonite) on the thermal decomposition of polypropylene sebacate (PPSeb). It was evidenced through the mass detection analysis of the generated decomposition compounds (aldehydes, alcohols, acids, etc.) that the PPSeb degradation involved mainly β-hydrogen bond scission and also α-hydrogen scission. The insertion of NPs led to the increase of the thermal stability of the polymer.146 Low-energy ion scattering (LEIS) is a modern analytical method that permits the rapid thickness characterization of self-assembled monolayers (SAM), for example, in the case of Au NPs. In this technique, a sample is exposed to low-energy gas ions, and the scattering and subsequent loss of energy of these ions can be related to the elemental composition of the outer layer surface.147 High sensitivity LEIS (HS-LEIS) offers better sensitivity for the investigation of distinct atomic layers with an extensive reduction in surface damage. HS-LEIS illustrated that a complete SAM was formed in the case of C16COOH-functionalized 14 nm Au NPs. The estimated SAM thickness was in good agreement with previous results from simulated electron spectra for the surface analysis of the XPS data. The LEIS thickness values were consistent with the values obtained by AFM, X-ray reflection and sputter depth profiling.147 The high sensitivity of HS-LEIS concerns the top ~10 nm of the surface atomic layers. This method is fast and rather direct, whereas SESSA simulations require a lengthy analysis of the results for the thickness, but can yield more information on chemical composition. Kauling et al. used HS-LEIS to analyse the outer layer of both functionalized and non-functionalized imidazolium ionic liquids on Au NPs. The description of its operation principle is described therein, together with its capacity to analyse the atomic composition and thickness of the surface of ionic liquids.148 Finally the formation of ruthenium–gold core–shell NPs prepared by the physical vapor deposition method on the TiO2 surface was studied by STM and LEIS, in an article published by Ovari et al. The chemical composition of the NPs was studied by LEIS, and it was found that when Rh was deposited on TiO2 previously covered by Au, Rh atoms impinged to Au clusters moved to subsurface sites; as a consequence, the outermost atomic layer of these clusters remained almost pure Au. STM and LEIS results showed that very limited mixing between Au and Rh in the bimetallic NPs took place (if any).149 UV-Vis spectroscopy (UV-Vis) is another relatively facile and low-cost characterization method that is often used for the study of nanoscale materials. It measures the intensity of light reflected from a sample and compares it to the intensity of light reflected from a reference material. NPs have optical properties that are sensitive to size, shape, concentration, agglomeration state and refractive index near the NP surface, which makes UV-Vis spectroscopy an important tool to identify, characterize and investigate these materials, and evaluate the stability of NP colloidal solutions.150 Gold, silver and copper nanostructure sols exhibit characteristic UV-Vis extinction spectra due to the existence of a LSPR signal in the visible part of the spectrum. In certain cases (e.g. metal chalcogenide NPs and anisotropic gold or silver nanostructures), LSPR bands at the near-infrared (NIR) wavelength region can also appear.151 Besides characterizing the NP optical properties, the size and molar concentration of zerovalent Au, for example, can also be obtained from the UV-Vis measurements. For this calculation, which can also be performed in situ under certain conditions, the position of the LSPR and the extinction at this wavelength, as well as the ratio of extinctions at the wavelength of the LSPR and at 450 nm (ALSPR/A450), are needed.151 The absorbance at 350–400 nm wavelength can also be used to measure the gold colloid concentration, however with an uncertainty up to 20–30% due to a rather slight influence of parameters such as NP size, surface modification and oxidation state. If these factors are taken into account upon calculation, the uncertainty in determining the Au NP concentration can be decreased extensively.151 In fact, the maximum absorbance at the UV-Vis spectra has also been successfully used for the calculation of the concentration of citrate-coated silver NPs.152 Haiss et al. have published a very high profile study on the utility of UV-Vis spectra to determine the size and concentration of Au NPs.153 The colloidal stability of Au NPs can be quantitatively characterized by UV-Vis absorbance spectroscopy, as shown by Pennathur and colleagues. Particle instability parameter (PIP) is a universal technique to quantitatively characterize the stability of plasmonic nanomaterials based on UV-Vis absorbance spectroscopy that does not depend on the colloid system and can fully record the evolution of a given studied system over time. It is a robust and generalizable approach, not only for Au NPs, but also for plasmonic NPs as a whole.154 Another use of UV-Vis spectroscopy involves the ability to detect molecules such as thiamine, by mixing a solution of thiamine in water with a Au NP solution. The presence of thiamine could be detected visually with a color change in the NP solution from red to greenish-grey. Au NPs tested for this application were in the range of 20–30 nm, whereas the limit of detection of thiamine was between 0.5 and 1 μM.155 In another report, Au and Pt NPs prepared by photoreduction synthesis in an aqueous medium containing dodecyltrimethylammonium chloride (DTAC) and PEG were studied by UV-Vis, EXAFS and other techniques (TEM, SAXS). EXAFS confirmed the metallic character of the NPs while SAXS implied that the structure of DTAC and PEG could be fitted with the hard-sphere model having the interaction radius (RHS) and the spherically shaped core–shell structure. The time evolution of the SAXS profiles was consistent with the UV-Vis spectral change during the first 30 min of photoirradiation.156 Behzadi et al. reported the development of a colorimetric sensor array to define the physicochemical properties of NPs dissolved in water with ultra-low concentrations. The effects of several dyes on different types of NPs were probed using variations in the visible spectrum of the dyes. The system should produce unique composite responses to each NP, similar to the well-established colorimetric array that is used to identify toxic chemical vapors.157 The authors prepared four different types of gold nanostructures and they employed their UV-Vis approach to detect and discriminate these particles. Overall, this method can be considered low-cost, non-destructive and quick for the recognition of NP systems and types. Ag nanostructures have also been extensively studied by UV-Vis spectroscopy. Jha and co-workers investigated the influence of maturing time and concentration of NaBH4 on size with UV-Vis. Their method, under the framework of the Mie theory, was employed to determine the particle size and size distribution. In fact, the LSPR of NPs is affected by size, shape, interparticle interactions, free electron density and surrounding medium, and this helps to obtain a screening of the electron injection and aggregation of NPs. In this way, it was possible to characterize the Ag NP formation kinetics and the final colloidal stability.158 In another work, Ag NPs were prepared via a green synthesis involving the flowers of the Moringa oleifera (MO) plant. This plant acted as a reducing and stabilizing agent, and the resulting particles were studied by FTIR, UV-Vis and other techniques. FTIR experiments demonstrated that proteins in the MO flower extract were adsorbed on Ag NPs, acting as capping agents. It also indicated that retinoic acid, a component of the MO flower extract, acted as a reductant. UV-Vis analysis verified the existence of LSPR in the produced particles and as the concentration of the MO flower extract increased, the absorption spectra showed a blue shift with decreasing NP size.159 Photoluminescence (PL) spectroscopy is another technique used to study nanoscale materials; it monitors the light emitted from atoms or molecules that have absorbed photons. PL is typically useful as the characterization technique for fluorescent nanoparticles, such as quantum dots, as well as metal nanoclusters. Recently, the inherent PL of metallic NPs received remarkable interest. Despite the fact that the quantum efficiency of the emission process is low, this inefficiency can be compensated by the large excitation cross sections at the plasmon resonances. In addition, the PL of metal NPs is free of photobleaching and photoblinking. Thus, PL can be regarded as a better alternative than fluorescent molecules for optical labeling applications. Single-photon and multi-photon excitation PL has been acquired using plasmonic nanostructures of several shapes.160 Gong and co-workers studied the PL behaviour of a single Au nanoflower, a highly branched plasmonic nanostructure. It was demonstrated that the PL measurements of such single Au nanoflower revealed some rather more complex features in comparison with simple nanostructures. Such PL properties of the Au nanoflower were strongly dependent on the excitation wavelength and polarization, and they were further studied in situ. The PL experiments and emission measurements comprised a complementary approach to the optical scattering method, and they are targeted to benefit potential applications in domains such as optical imaging and sensing.160 Andersen et al. illustrated the PL wavelength and polarization engineering by exploiting arrayed Au NPs atop a subwavelength-thin dielectric spacer and optically thick Au film, a configuration that supports gap-surface plasmon resonances.161 On the other hand, quantum dots such as metal chalcogenide NPs have widely been studied by PL. For instance, the extinction and photoluminescence of Cu2−xS, Cu2−xSe and Cu2−xTe NPs have been investigated by Feldmann and co-workers and the tunability and control over those properties have been discussed through the active manipulation over their copper deficiency under oxidative/reductive conditions. It was demonstrated that the presence of NIR LSP resonances in these NPs had a crucial effect on the exciton recombination. For example, the PL of Cu2S nanoclusters was quenched during their gradual transformation to non-stoichiometric nanoclusters (x > 0) under an oxidative environment.162 Metal oxides such as ZnO NPs are also photoluminescent. Saliba et al. synthesized zinc oxide NPs in the presence of branched thermotropic liquid crystals. Three emissions were observed for their particles, depending on the excitation wavelength. The origin of such emissions was attributed to several factors, such as surface defects (e.g. oxygen vacancies).163 Another example of nanoscale materials with photoluminescent properties is cesium lead halide perovskites. Protesescu et al. synthesized cesium lead halide nanocrystals using inexpensive commercial precursors and they studied their photoluminescence properties. The colloidal CsPbX3 (X = Cl, Br, I and mixed Cl/Br, Br/I) NPs were bright (quantum yield = 50–90%), stable, and spectrally narrow and had tunable bandgap energies.164 Dynamic light scattering (DLS) is a widely employed technique to find the size of NPs in colloidal suspensions in the nano- and submicrometer ranges. The NPs dispersed in a colloidal solution are in continuous Brownian motion. DLS measures light scattering as a function of time, which combined with the Stokes–Einstein assumption are used to determine the NP hydrodynamic diameter (i.e. diameter of the NP and the solvent molecules that diffuse at the same rate as the colloid) in solution. In DLS, a relatively low NP concentration is needed so that a multiple scattering effect is avoided.165 Lim et al. have reviewed the characterization of NPs by DLS (Fig. 2) focusing in the case of magnetic particles. They present how various factors such as suspension concentration, particle shape, colloidal stability and surface coating of MNPs influence the size value obtained by DLS measurements. A comparison between the results derived from DLS and other techniques, such as TEM and AFM, is performed and the origins for any discrepancies in the sizing, for either small or larger particles, are discussed, while the working size range for each technique is also given.166 For example, for small-sized NPs, the radius of curvature effect is the principal contributing factor for the large difference observed for the diameter measured by TEM and DLS. Middle-sized Fe3O4 NPs capped with oleic acid and oleylamine seem to have size values that show the best match among DLS and TEM measurements. The authors highlight the use of DLS also for the measurement of the colloidal stability of MNPs. Moreover, DLS has been proven useful to monitor the transient behaviours of β-FeOOH nanorods: these structures self-assemble in a side-by-side fashion to form highly oriented 2-D nanorod arrays, eventually leading to the formation of 3-D layered architectures. Overall, the real-time screening of NPs by DLS provides important insights into their aggregation process, since it measures quantitatively the size of the particle clusters formed. The sensitivity of DLS to large particles is crucial for its excellent diagnostic capability to detect aggregation.

Nevertheless, the authors denote that careful analysis is required for the best possible interpretation of the DLS results as they are affected by the factors previously mentioned (shape, coating agents, etc.).166 The advantages of DLS include its quick, easy and precise operation for monomodal suspensions and the fact that it is an ensemble measurement method, yielding a good statistical representation of each NP sample. It is highly sensitive and reproducible for monodisperse, homogeneous samples. A limitation of DLS is the necessary conditions for the particles to be in suspension and undergoing Brownian motion. Large particles scatter much more light and even a small number of large particles can obscure the contribution from smaller particles. Therefore, its resolution for polydisperse, heterogeneous samples is rather low. DLS requires transformative calculations with assumptions that must be taken into account when interpreting the data – particularly with polydisperse samples. Although DLS can sometimes measure anisotropic nanostructures, it generally assumes spherical shaped particles.167,168 Overall, DLS measures the hydrodynamic radius accurately but lacks the resolution to detect small aggregates. However, when coupled with differential centrifugal sedimentation (DCS), for example, it can result in valuable information for core–shell NPs, as in the case of those prepared by Minelli and co-workers: when DCS confirms that the samples are not aggregated, the measurements by DLS can be safely considered as accurate.169 Coleman et al. have compared several methods used to obtain information on particle size distributions. For instance, if ~1% of larger particles exist in a sample, in comparison with the majority of the particles (e.g. two-fold or three-fold larger than the average size of 99% of the particles), DLS is significantly affected, giving higher values than TEM (e.g. 42 nm for a given silica reference sample compared to 25 nm by TEM). Moreover, DCS, apart from its above-mentioned ability to detect agglomerate clusters, is able to characterize samples with broad size distributions.170 Fig. 2 Optical configuration of the typical experimental setup for dynamic light measurements of a nanoparticle suspension. The setup can be operated at multiple angles. Reproduced with permission from ref. 166. Copyright 2013 Springer. Driskell and co-workers employed DLS to elaborate a fast one-step screening method for the characterization of the specificity of antibody–antigen binding using antibody-conjugated Au NPs. The advantages of DLS detection over the more classic colorimetric technique include better detection limits and higher sensitivity. DLS was used to measure the formation of aggregates produced from virus–antibody binding. The extent of aggregation was employed to assess the interaction between the antibody and the virus. Their novel approach offers an important improvement regarding screening time in comparison with ELISA assays, while giving similarly precise results as the conventional method.171 DLS has also been combined with DOSY- and NOESY-NMR techniques to explore the partitioning behaviour of secondary surfactants added to suspensions of reverse micelles containing either Au or Ag NPs. The critical role of NPs and the surfactant amount on the efficiency of surfactant-assisted NP extraction was investigated. Examples of the surfactants tested were oleylamine, oleic acid and dodecanethiol. The average particle diameters acquired by TEM imaging were lower than those measured by DLS, since the DLS values reflect the outer diameter of the NP-containing AOT reverse micelles together with any related solvent molecules. DLS helped in the monitoring of the irreversible penetration of reverse micelles by specific secondary surfactants.172 Fissan et al. used an aerosol technique, named scanning mobility particle sizer (SMPS), to characterize Au-PVP and Ag-PVP NPs and they compared these results with the ones obtained from techniques such as SEM and DLS. For samples with binary dispersion, DLS failed to provide a correct feedback on the particle size, whereas SEM, SMPS and analytical disk centrifugation (ADC) managed to identify the two different particle size populations. In particular, ADC has a high resolution and can distinguish mixtures if the components cover different size ranges or have distinct densities. ADC is though time-consuming in some cases and it can somewhat underestimate the NP size. Combining SMPS with a nebulizer may result in a method with a higher resolution than ADC.173 Grobelny and co-workers investigated the size and size distribution of polydisperse silver NP colloids using DLS and UV-Vis. Although DLS is more sensitive than UV-Vis, its usual drawback has to do with the difficulty in detecting the presence of smaller NPs; in addition, the UV-Vis spectra did not contain any separate peaks for NPs of different sizes. Therefore, the authors concluded that UV-Vis should not be used for size determination in the case of polydisperse samples. UV-Vis and DLS are low-cost and fast methods, but care is needed when interpreting their results, especially for the aforementioned types of samples, which do not contain a single NP population. Complementary measurements with AFM and TEM/SEM will be certainly needed for polydisperse samples.174 Kestens et al. used numerous techniques (DLS, CLS, SEM, TEM, AFM, and PTA) to measure the size of a 'standard' SiO_2 nanomaterial sample. Measurements from several researchers working in distinct laboratories were studied. The authors presented the nanomaterial tested as a new reference material with certified values and uncertainties that can be used for assessing the reliability of several particle size analysis methods.175 Murdock et al. characterized a broad range of nanomaterials in solution using DLS and TEM, before assessing their in vitro toxicity. Metal and metal oxide NPs, such as Al, Al_2O_3, SiO_2 and Cu NPs, as well as carbon-based materials such as carbon nanotubes, were tested. DLS measurements showed that depending on the material examined, when the NPs are in solution they do not necessarily retain their nanoscale size.176 Nanoparticle tracking analysis (NTA) is a relatively new, but quickly adopted, technique that can measure NP size, and having a lower concentration detection limit compared to DLS. It utilises the properties of both light scattering and Brownian movement so as to acquire a NP size distribution of samples in liquid dispersion. The details of its operation principle (Fig. 3) and further technical information are provided by Hole et al.177 That paper examined the reproducibility of results acquired by NTA by investigating a wide range of nanoparticle systems and size ranges, in different media. The measurements were performed in 12 distinct laboratories, aiming to obtain a wide database. Examples of the types of nanomaterials tested were Au, SiO_2 and polystyrene NPs, dispersed in water or in biological media. An important advantage that NTA offers in comparison with other size measurement techniques is that it is not biased toward larger NPs or aggregates. Furthermore, its confirmed accuracy and reproducibility verified the suitability of NTA to determine the size populations of bimodal samples. The comparison between NTA and DLS was also examined by Jiskoot and colleagues, investigating standard polystyrene beads in the size range of 60–1000 nm.178 Physical mixtures of samples with different NP sizes were also evaluated. It was shown that NTA yielded precise values for the size distribution of both monodisperse and polydisperse samples. The average size values recorded by NTA were slightly smaller and more exact to the nominal ones than those obtained by DLS. Nevertheless, NTA is slower and has a somewhat more difficult operation mode compared to DLS. That study corroborated the above-mentioned findings of other researchers which mention that DLS results are not easily interpreted in the case of polydisperse samples, whereas NTA is able to identify two different sample populations in the same sample.178 Overall, NTA tracks single particles, while DLS studies an ensemble of particles and it is strongly biased to the biggest particles, which are present in the sample. NTA was also studied by Hassellov and co-workers for its capacity to determine the size distributions and concentrations of NPs in liquid samples. Apart from the differences among DLS and NTA, the authors concluded that NTA allows the measurement of large amounts of particles, compared to TEM. Therefore, the statistical confidence is increased and the absence of any particle changes because of the preparation mode of the specimen tested is ensured. Additionally, NTA can potentially use the intensity of light scattered by individual particles to discriminate particles composed of distinct materials within a given size range.179 It is important to note that the sensitivity of NTA is related to the size and composition of the nanomaterials studied. In another report, Ryu et al. prepared $CaWO_4$ and $CaMoO_4$ NPs via the pulsed laser ablation method, and they used several techniques to characterize them, including NTA. The latter technique can dynamically analyse the paths the NPs take under Brownian motion over a suitable time range (e.g. 10–20 s) and visualize deeply sub-micron particles in real time and in a liquid medium. NTA combined with image analysis determined the particle size distribution function of the aforementioned samples. The results for the mean NP size were in accordance with the values derived by TEM and XRD.180 Fig. 3 Schematic of the optical configuration used in NTA. Reprinted with permission from ref. 177. Copyright Springer 2013. NTA has also been employed to analyse the capping efficiencies of several biomass-derived stabilizers of colloidal Ag suspensions in water. The NTA software identifies and tracks single NPs that undergo Brownian motion and correlates the velocity of the movement with the NP size. For instance, bigger NPs and heavy aggregates move with a slow speed, in comparison with smaller NPs, which have less weight and move faster. It was found that a biorefinery-derived residual syrup acted as an efficient stabilizing agent for silver NPs in solution.181 Another use of NTA, presented by van Leeuwen and co-workers, is the determination of the refractive index which dictates the interaction between light and NPs. Heterogeneous NPs were tested, with sizes